Chemistry–A European Journal
Research Article
doi.org/10.1002/chem.202200786
Chemistry Europe
European Chemical Societies Publishing
www.chemeurj.org

Synthesis and Biological Evaluation of Flavonoid-Cinnamic Acid Amide Hybrids with Distinct Activity against Neurodegeneration in Vitro and in Vivo

Julian Hofmann,[a] Philipp Spatz,[a] Rasmus Walther,[a] Marcus Gutmann,[b] Tangui Maurice,[c] and Michael Decker*[a]

Abstract: Flavonoids are polyphenolic natural products and have shown significant potential as disease-modifying agents against neurodegenerative disorders like Alzheimer's disease (AD), with activities even in vivo. Hybridization of the natural products taxifolin and silibinin with cinnamic acid led to an overadditive effect of these compounds in several phenotypic screening assays related to neurodegeneration and AD. Therefore, we have exchanged the flavonoid part of the hybrids with different flavonoids, which show higher efficacy than taxifolin or silibinin, to improve the activity of the respective hybrids. Chemical connection between the flavonoid and cinnamic acid was realized by an amide instead of a labile ester bond to improve stability towards hydrolysis. To investigate the influence of a double bond at the C-ring of the flavonoid, the dehydro analogues of the respective hybrids were also synthesized. All compounds obtained show neuroprotection against oxytosis, ferroptosis and ATP-depletion, respectively, in the murine hippocampal cell line HT22. Interestingly, the taxifolin and the quercetin derivatives are the most active compounds, whereby the quercetin derivate shows even more pronounced activity than the taxifolin one in all assays applied. As aimed for, no hydrolysis product was found in cellular uptake experiments after 4 h whereas different metabolites were detected. Furthermore, the quercetin-cinnamic acid amide showed pronounced activity in an in vivo AD mouse model at a remarkably low dose of 0.3 mg/kg.

Introduction

In 2003, Przedborski et al. defined neurodegeneration as "any pathological condition primarily affecting neurons".[1] Neuronal damage leads to cognitive disfunction, impaired memory and finally to the loss of brain function.[2] Neurodegeneration plays a central role in chronic diseases like Alzheimer's disease (AD) and there is no treatment yet available to prevent or slow down the progression of the disease.[3] Major risk factors for neurodegeneration are age, genetic risks, and environmental factors, which are thought to initially disturb cell homeostasis.[4] The imbalance in cell homeostasis leads to mitochondrial dysfunction, oxidative stress and inflammation, enhancing neurodegeneration and disease progression.[4] Due to the complexity of neurodegeneration, multi-target directed ligands have drawn the attention of current research.[5] Secondary plant metabolites, commonly known as natural products, are important for drug discovery and many derivatives are promising candidates as lead structures for disease modifying agents against neurodegeneration (for detailed reviews, cf. Ref. [3,5,6]).[3,5,6] In particular, flavonoids, a group of polyphenolic natural products, have shown a remarkable properties as potentially disease-modifying agents in phenotypic screening assays as well as in animal models.[7] Recent studies have shown that hybridization of both the flavonolignan silibinin and the flavanonol taxifolin with different aromatic and phenolic acids could increase their neuroprotective potency significantly.[8] The compound 7-*O*-cinnamoyltaxifolin (cf. Figure 1.)[8b] showed pronounced overadditive effects against oxytosis, ferroptosis and ATP-depletion and by converting the parent compound into a chemical probe with an alkine tag revealed the adenine nucleotide translocase 1 (ANT-1) and sarco/endoplasmic reticulum Ca^{2+} ATPase (SERCA) as specific interaction partners in activity-based protein profiling.[9] Hybridization was achieved by esterification, however in case of the silibinin esters the molecules were fairly unstable due to hydrolysis in cell culture medium.[10] No

[a] *Dr. J. Hofmann, P. Spatz, R. Walther, Prof. Dr. M. Decker*
Pharmaceutical and Medicinal Chemistry
Institute of Pharmacy and Food Chemistry
University of Würzburg
Am Hubland, 97074 Würzburg (Germany)
E-mail: michael.decker@uni-wuerzburg.de

[b] *Dr. M. Gutmann*
Drug Formulation and Delivery
Institute of Pharmacy and Food Chemistry
University of Würzburg
Am Hubland, 97074 Würzburg (Germany)

[c] *Dr. T. Maurice*
MMDN
University of Montpellier, EPHE, INSERM
34095 Montpellier (France)

Supporting information for this article is available on the WWW under https://doi.org/10.1002/chem.202200786

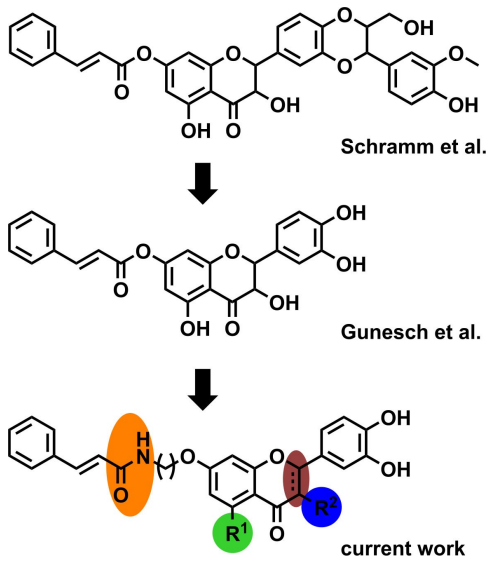

Figure 1. Compound development of flavonoid-cinnamic acid amide hybrids.[8a,b] Yellow: Amide-linker; green and blue: hydroxylation pattern, brown: dehydro-site.

hydrolysis product was found for the taxifolin esters, but nevertheless nearly no compound was detectable by HPLC analysis after 4 hour incubation in cellular uptake experiments.[8b] These uptake experiments also revealed the conversion of 7-*O*-cinnamoyltaxifolin to 7-*O*-cinnamoylquercetin, leading to the question, which of the compounds is actually responsible for the biological response.[8b] Herein, a small library of six flavonoid-cinnamic acid derivates was synthesized. The connection between the flavonoid and cinnamic acid was achieved via an amide linker to prevent hydrolysis. The synthesis was accomplished based on per-*O*-acetylation of the flavonoids followed by regioselective deprotection of the 7-OH group, which made the compound accessible for connection with cinnamic acid.[11] The library consists of three pairs of a flavanone and the respective flavone to investigate the influence of the double bond at the C-ring on biological activity (cf. Figure 2.). Because of the pleiotropy of neurodegeneration, the compounds were tested in several phenotypic screening assays in the murine hippocampal cell line HT22.[12] The compounds were investigated in cellular uptake experiments regarding putative chemical transformations and stability in cell culture medium was assessed. Finally, in vivo investigations into an AD mouse model with Ab_{25-35}-induced memory impairment were conducted.[13]

Results

Synthesis of flavonoid cinnamic acid amides

Synthesis of the desired target compounds was achieved either synthetically or semi-synthetically, starting from a commercially available flavonoid (Figure 2.). To obtain the flavanones fustin and eriodictyol, common synthetic procedures for flavonoids were applied.[14] Condensation of a methoxymethyl (MOM)-protected acetophenone with MOM-protected 3,4-dihydroxy benzaldehyde yielded the respective chalcone (cf. Schemes 1 and S1). Oxidation of the double bond of the respective chalcone with hydrogen peroxide under basic conditions led to an epoxide, which served as the precursor of the hydroxy group at C-3 of fustin.[15] Heating in 10% hydrogen chloride in MeOH cleaved the MOM-groups and simultaneously formed the flavonoid. For luteolin, acetylation followed by dehydrogenation with *N*-bromosuccinimide (NBS) in the presence of catalytic amounts of azobisisobutyronitrile (AIBN) gave per-*O*-acetyl luteolin.[16] Taxifolin, quercetin and fisetin were purchased from commercial suppliers. After per-*O*-acetylation with acetic acid anhydride in the presence of catalytical amounts of iodine, the flavonoids were selectively deprotected at C-7 as described in a procedure by Mattarei et al.[11] with imidazole. Afterwards, they were connected to the cinnamic acid amide via Williamson

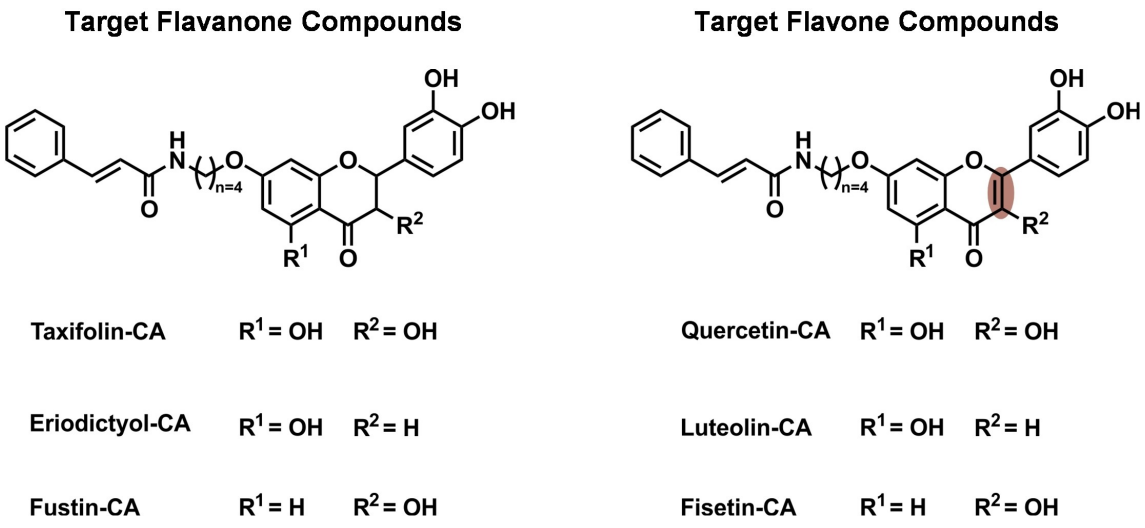

Figure 2. Overview target flavanone and flavone compounds. Flavones carry a double bond within the C-ring (highlighted). CA = cinnamic acid amide.

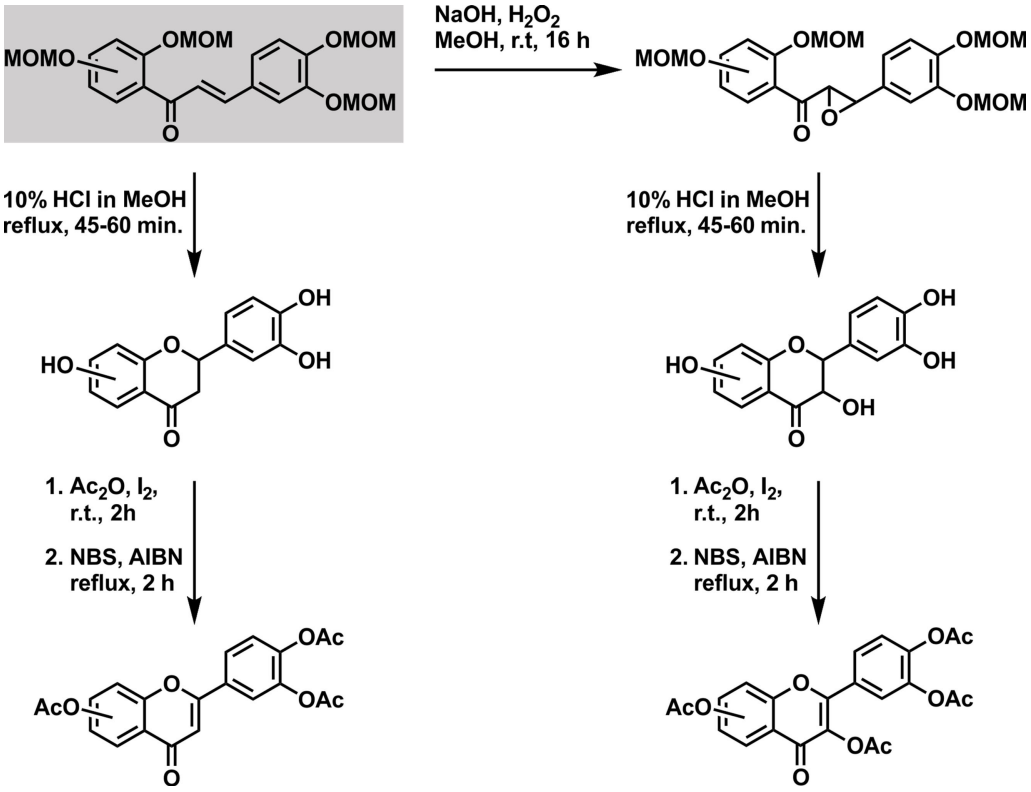

Scheme 1. General synthesis of per-*O*-acetyl flavonoids starting from a chalcone (highlighted).

ether synthesis, directly followed by deprotection with 6 M hydrogen chloride in acetonitrile (cf. Scheme 2.).

Neuroprotection in HT22 cells - oxytosis

Oxidative glutamate toxicity (oxytosis) is a non-excitotoxic pathway for programmed cell death, which was examined in the murine neuronal cell line HT22 (Figure 3).[17] Oxytosis shares many physiological and morphological features with nerve cell death observed in AD and generality of this pathway makes it a well suitable assay for initial screening of potentially neuroprotective compounds.[18] Excess of extracellular glutamate inhibits the cystine/glutamate antiporter system X_c^- and leads to glutathione (GSH) depletion. Upon low levels of GSH (reached within 6–8 hours after glutamate treatment), reactive oxygen species (ROS) rise exponentially and over a subsequent cascade, cell death is induced.[17a,18] For every cellular assay, toxicity data of the compounds themselves needs to be taken into account (cf. Figure S1), because concurrent effects of the insult (glutamate, RSL-3 or IAA) and the compounds may show up. All compounds tested showed protection against gluta-

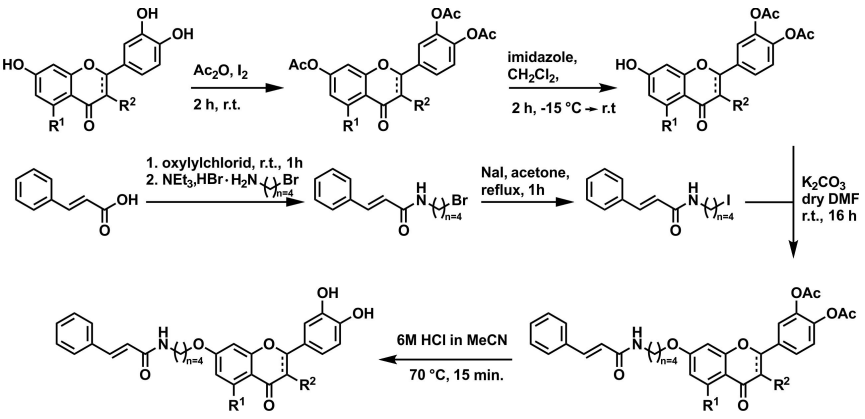

Scheme 2. General synthesis of flavonoid-cinnamic acid amides.

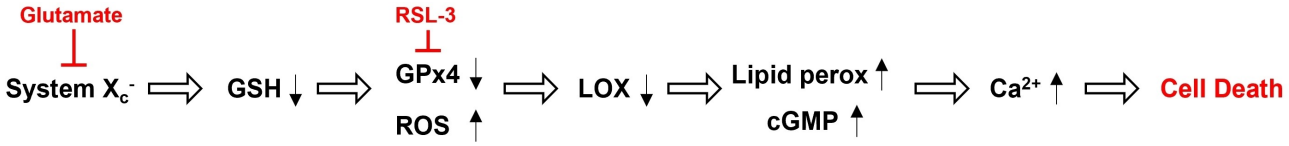

Figure 3. Overview oxytosis/ferroptosis pathway.

mate-induced cell death and the quercetin derivative was the most active compound at a concentration of 1.56 μM (Figure 4). Interestingly, the quercetin-CA was at one lower concentration level active than the taxifolin derivate. The eriodictyol derivative showed greater protection than the luteolin one (3.12 μM vs. 6.25 μM) and the fustin derivative showed comparable results to the fisetin one. Overall, there was no clear trend in the oxytosis assays with regards to a significant difference in the biological activities of the amide hybrids of flavanones and the flavones, respectively.

Quantification of reactive oxygen species (ROS)

As discussed above, there is a time dependent accumulation of ROS 6–8 h after glutamate treatment (Figure 3).[17a,18] The ROS accumulation happens downstream of the cystine/glutamate antiporter X_c^- and quantification of ROS therefore gives additional information, at which state of the oxytosis cascade the compounds may act. Importantly, ROS do not kill the cells directly, but activate a number of downstream events leading to cell death.[19] The reduced fluoresceine derivate CM-H_2DCFDA is a versatile oxidative stress indicator and a fluorogenic probe, which evolves its fluorescence after oxidation by ROS (Figure 5).[20] Both the taxifolin and the quercetin amide hybrids were investigated regarding an influence on ROS accumulation. The quercetin derivative could indeed prevent glutamate-

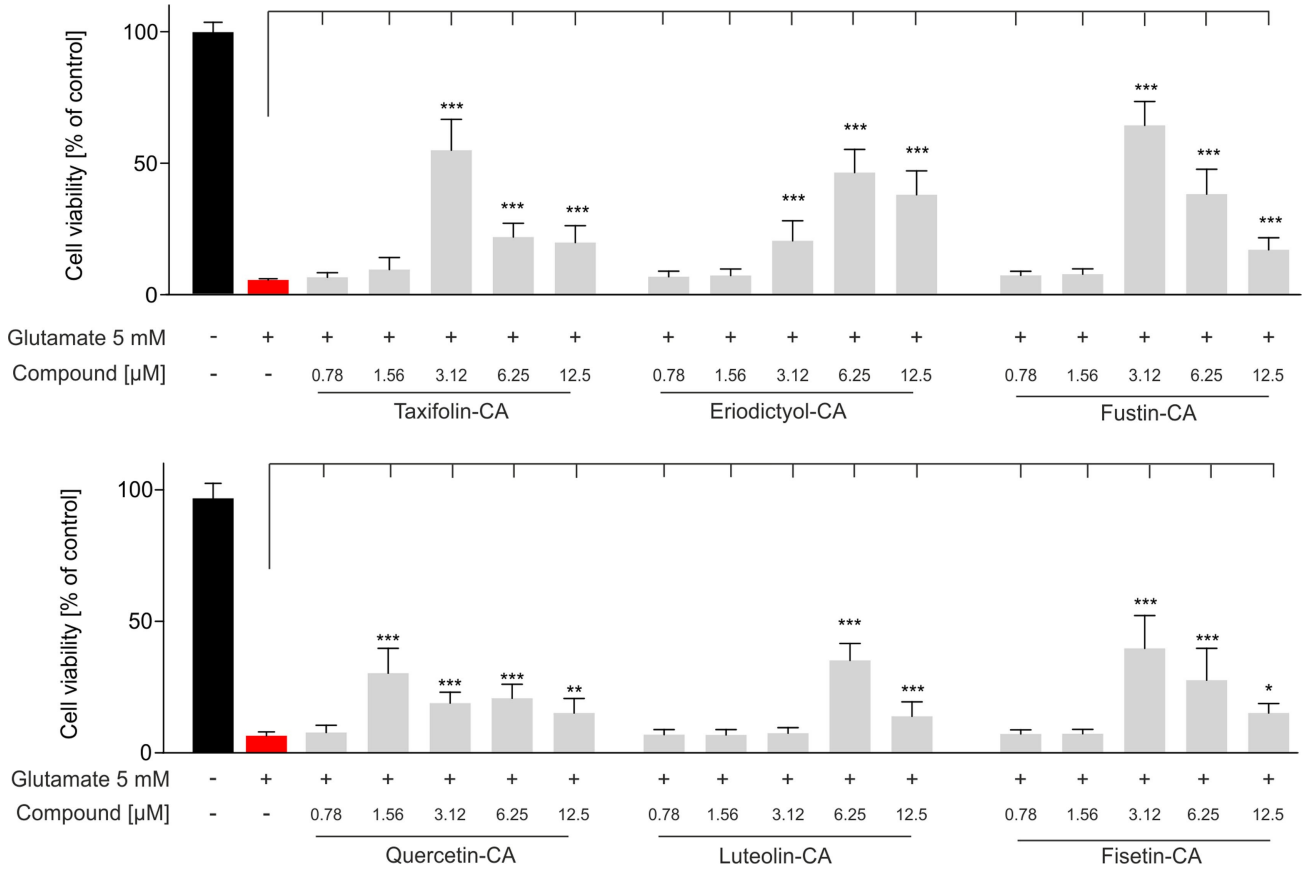

Figure 4. Oxytosis assay in murine hippocampal HT22 cells. Cells were treated with 5 mM of glutamate alone (red) or in the presence of the indicated compound (grey). Data are presented as means ± SEM of three independent experiments and results refer to untreated control cells (black). Statistical analysis was performed using One-Way ANOVA followed by Dunnett's multiple comparison posttest using GraphPad Prism 5 referring to cells treated with 5 mM of glutamate. Level of significance: *$p < 0.05$; **$p < 0.01$; ***$p < 0.001$.

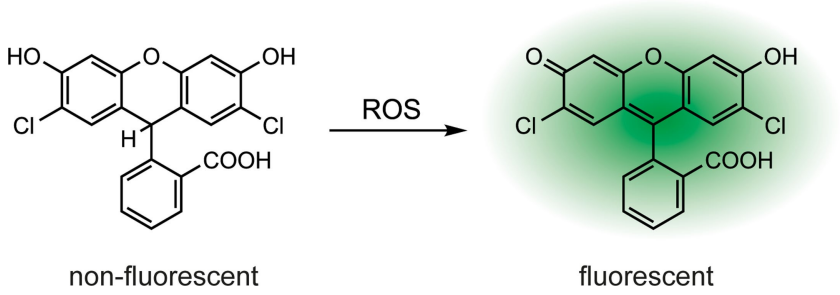

Figure 5. General scheme for a fluorogenic probe, i.e., the reaction of a non-fluorescent fluoresceine derivative with reactive oxygen species (ROS) to a fluorescent dye.

induced ROS accumulation at 1.56 μM, whereas taxifolin-CA did not (Figure 6A and C). These results are consistent with the activities found in the oxytosis assay and indicated, that the compounds could even decrease the basal level of ROS. Thus, the influence of the two hybrids on HT22 cells without prior exposure to glutamate was investigated (Figure 6B). Both compounds decreased the basal level of oxidative stress in HT22 cells, the quercetin hybrid decreased basal ROS significantly already at 3.12 μM, whereas the taxifolin derivative showed statistically significant activity only at 12.5 μM.

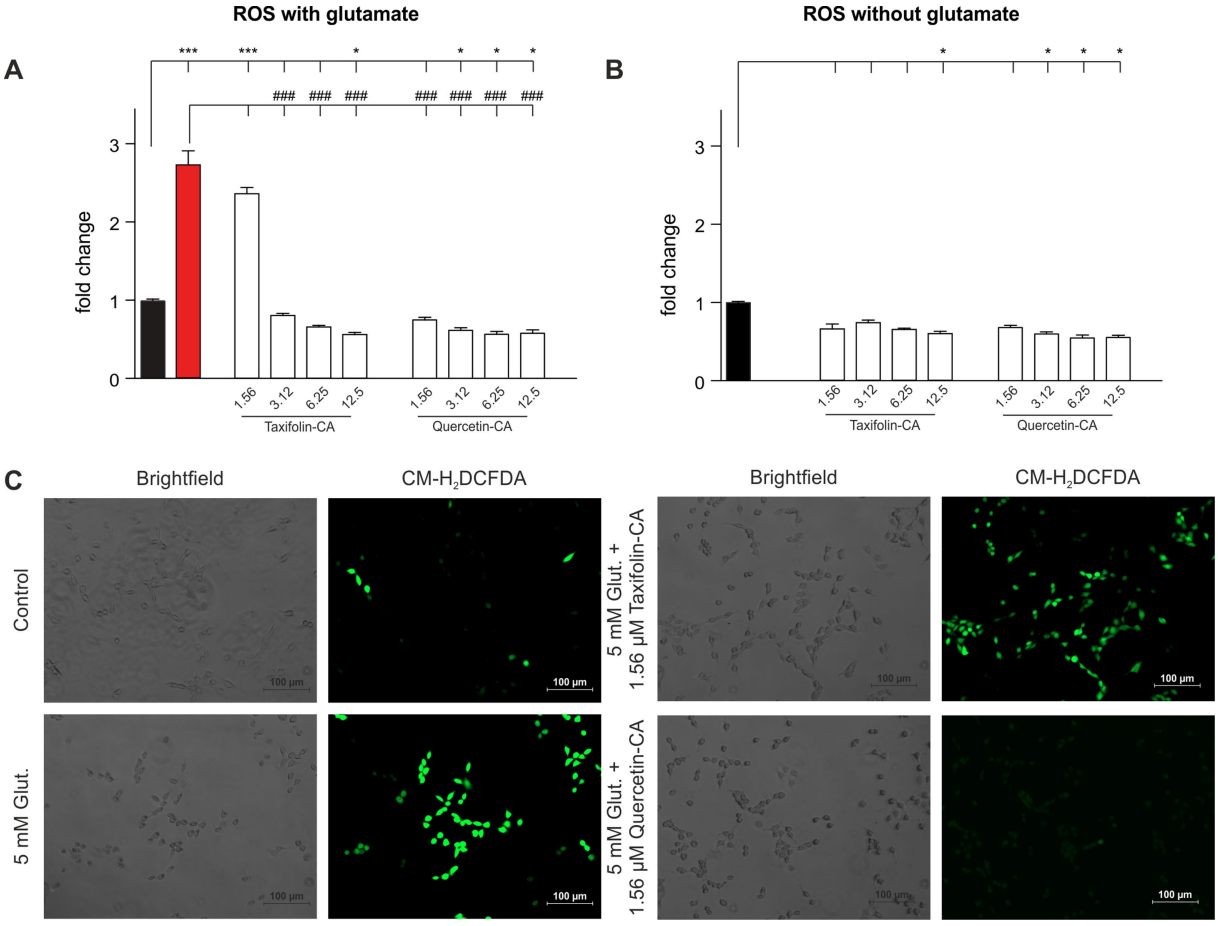

Figure 6. Qualitative and quantitative analysis of formation of reactive oxygen species (ROS) with CM-H_2DCFDA in HT22 cells. The cells were treated with (red) or without glutamate (black) for 6 h in the presence or absence of taxifolin-CA and quercetin-CA (white). A) Dose dependent effect of taxifolin-CA and quercetin-CA on glutamate-induced ROS-levels, B) dose dependent effect of taxifolin-CA and quercetin-CA on basal ROS levels, C) visualization of glutamate-induced ROS via fluorescence microscopy at a compound concentration of 1.56 μM. Statistical analysis was performed using One-Way ANOVA followed by Dunnett's multiple comparison posttest using GraphPad Prism 5 referring to untreated control cells (*) or cells treated with 5 mM of glutamate (#). Level of significance: */# $p < 0.05$; **/## $p < 0.01$; ***/### $p < 0.001$.

Neuroprotection in HT22 cells - ferroptosis

Ferroptosis is closely related to oxytosis. RSL-3 is an inhibitor of glutathione peroxidase 4 (GPx4), a GSH-dependent antioxidant enzyme. This enzyme acts quite in the middle of the oxytosis/ferroptosis pathway (Figure 3). The depletion of GSH in oxytosis assays leads to loss of activity of GPx4, in the ferroptosis assay it is directly inhibited by RSL-3.[19] All compounds tested were neuroprotective against ferroptosis (Figure 7). Again, taxifolin-CA and quercetin-CA were the most active compounds and quercetin-CA was also active at one concentration level lower than the taxifolin hybrid. Fustin-CA and fisetin-CA showed comparable results, both were active at 6.25 μM. Interestingly, the eriodictyol and luteolin hybrids changed their activity profile. In the oxytosis assay, luteolin-CA showed neuroprotection at 6.25 μM and eriodictyol-CA at 3.12 μM. In the ferroptosis assay, the lowest active concentration of luteolin-CA was 3.12 μM.

Protection of energy loss in HT22 cells

Breakdown of energy production and decrease of ATP levels in the brain is associated with neuronal damage and neurodegeneration.[21] Therefore, compounds which maintain ATP levels are of interest as treatment options of neurodegenerative diseases. To induce the loss of ATP, HT22 cells were treated with iodoacetic acid (IAA), an irreversible inhibitor of the enzyme glyceraldehyde 3-phosphate dehydrogenase (GAPDH), which is a key enzyme in glycolysis for energy production.[22] As for oxytosis and ferroptosis assays, as well as in the ROS accumulation assay, the cinnamic acid amide flavonoids hybrids rescued the cells from death (Figure 8). Furthermore, taxifolin-CA and quercetin-CA were the most active compounds and like in the other assays, quercetin-CA was more active than taxifolin-CA (3.12 μM vs. 6.25 μM).

Stability in cell culture medium and cellular uptake studies

Prior to cellular uptake experiments, the stability of taxifolin-CA was assessed in assay medium. The hybrid compound was

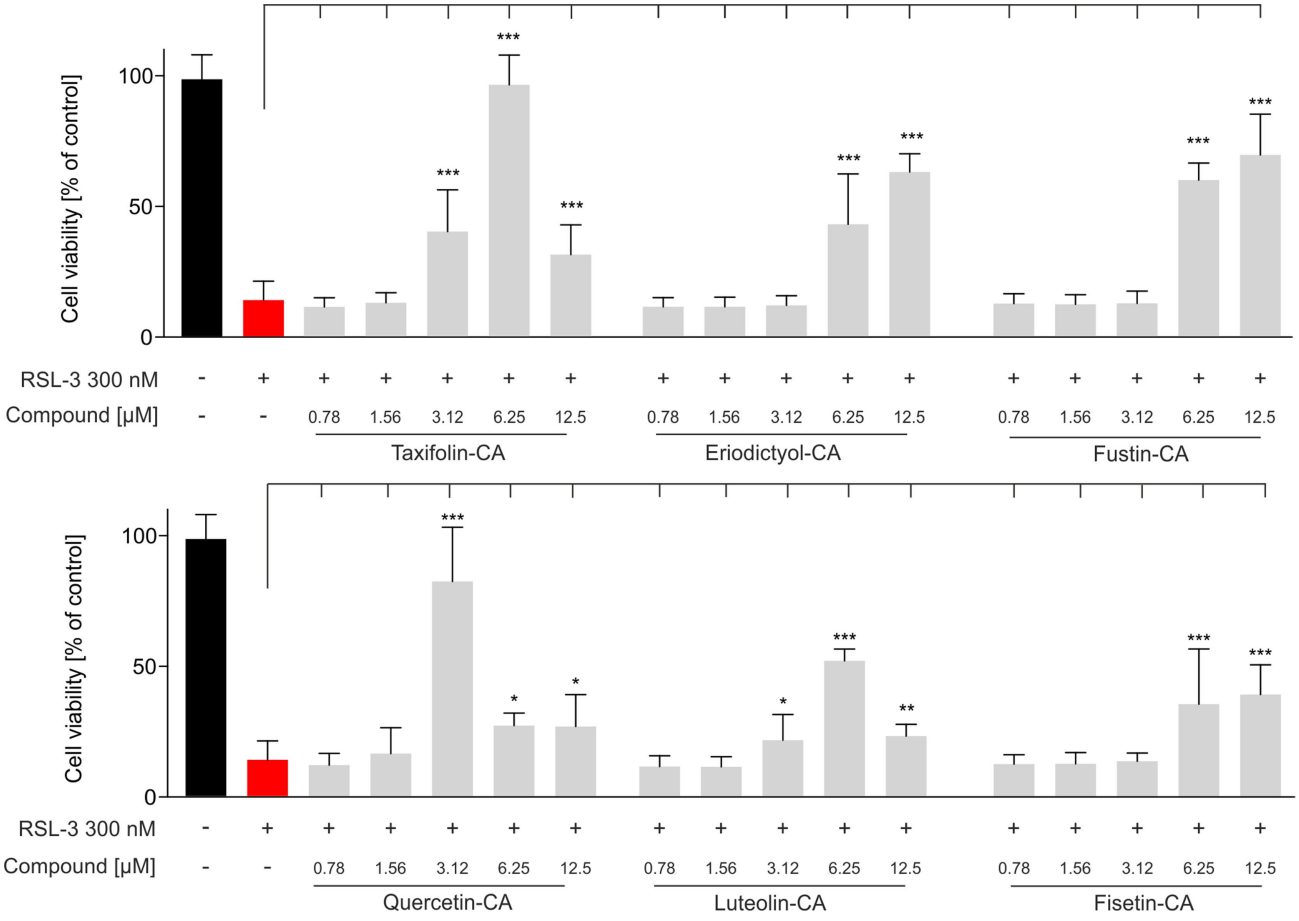

Figure 7. Ferroptosis assay in murine hippocampal HT22 cells. Cells were treated with 300 nM of RSL-3 alone (red) or in the presence of the indicated compound (grey). Data are presented as means ± SEM of three independent experiments and results refer to untreated control cells (black). Statistical analysis was performed using One-Way ANOVA followed by Dunnett's multiple comparison posttest using GraphPad Prism 5 referring to cells treated with 300 nM of RSL-3. Level of significance: *$p < 0.05$; **$p < 0.01$; ***$p < 0.001$.

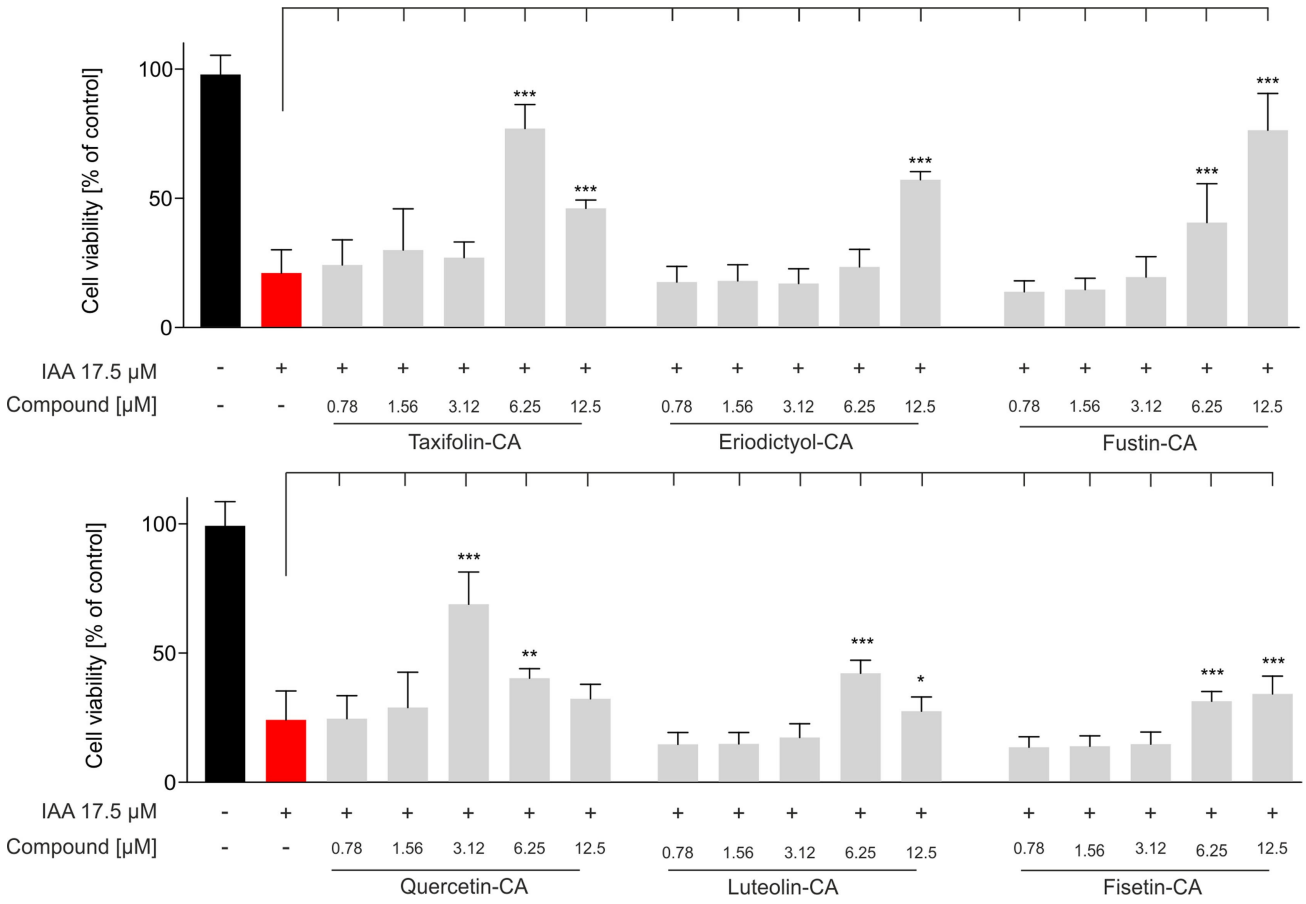

Figure 8. ATP-depletion was induced with 17.5 µM of IAA in the absence (red) or presence of the indicated compound (grey). Data are presented as means ± SEM of three independent experiments and results refer to untreated control cells (black). Statistical analysis was performed using One-Way ANOVA followed by Dunnett's multiple comparison posttest using GraphPad Prism 5 referring to cells treated with 17.5 µM of IAA. Level of significance: $*p<0.05$; $**p<0.01$; $***p<0.001$.

incubated at 37 °C in cell culture medium and analyzed by LC-UV/MS. No specific degradation product was found, however, the compound's concentration decreased over time to 54.6% of the initial concentration after 4 h (Table 1). It was described that taxifolin-aromatic acid hybrids can be oxidized to the respective quercetin derivatives in the presence of BV-2 microglia or RAW264.7 macrophages.[8b,c] Therefore, we conducted cellular uptake experiments for more detailed information about the intracellular metabolism of taxifolin-CA. Microglial BV-2 cells were treated for 0 h to 4 h before cell lysis and LC-UV/MS analysis (Figure 9). Quantification of the intracellular taxifolin-CA concentration was achieved by using a calibration curve and standard as well as by a blank chromatogram (cf. Supporting Information). The maximal intracellular concentration of taxifolin-CA was reached after 0.5 h at a concentration of 3.4 µM. Besides the chromatographic peak of taxifolin-CA at retention time 21.9 min (red) with *m/z* 506.1, three prominent peaks formed at 22.7 min (blue), 24.2 min (orange) and 25.4 min (green), respectively. Mass spectroscopic analysis showed molecular ions $[M+H]^+$ with *m/z* 520.15 for the blue peak, *m/z* 504.05 for the orange one, and *m/z* 518.15 for the green one. The *m/z* 504.05 and retention time of 24.2 min (orange) refer to the quercetin-CA derivative. Compared to literature data,[8b,c] the conversion rate of the taxifolin hybrid to the quercetin hybrid is much lower. The masses *m/z* 520.15 and *m/z* 518.15 may refer to the methylated taxifolin, or quercetin hybrid, respectively. Similar results were obtained in HT22 cells (cf. Supporting Information).

Table 1. Stability of taxifolin-CA in cell culture medium. The compound was dissolved in DMSO, diluted into cell culture medium, and incubated for the indicated time period prior to LC/MS analysis.

Time [h]	Amount [%]	SEM
0	100.0	0.0
0.5	88.8	6.1
1	82.1	8.7
2	70.5	6.9
4	54.6	3.0

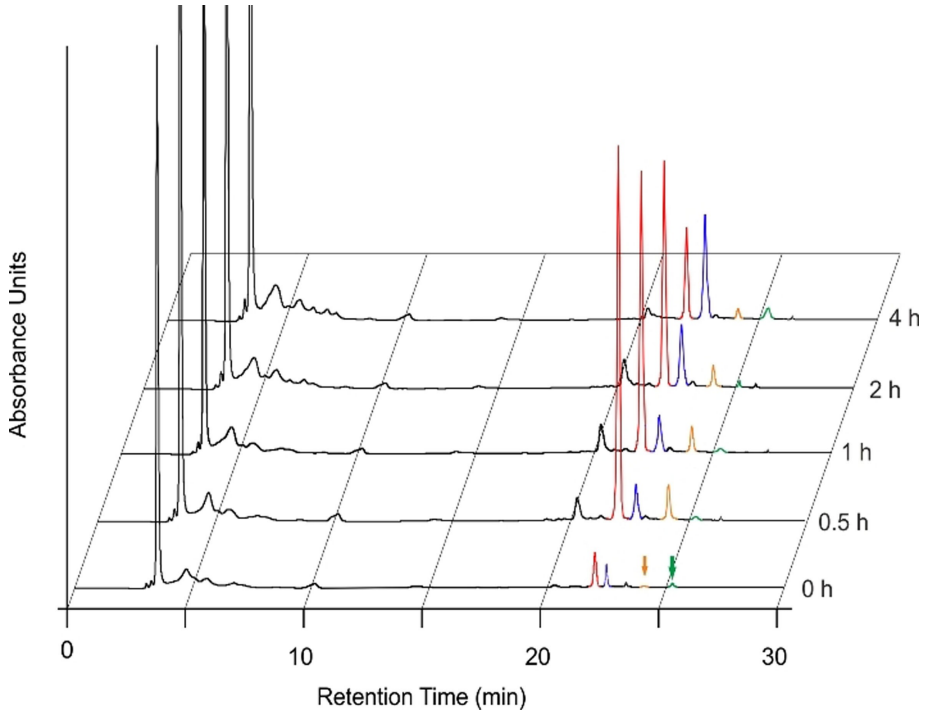

Figure 9. Chromatogram overlay of cellular uptake experiments for taxifolin-CA. BV-2 cells were treated for the indicated time period with 50 μM of taxifolin-CA. Taxifolin-CA (red) was converted into quercetin-CA (orange) and both compounds show a conversion to a compound being one methyl group heavier (m/z + 15.0) than the parent compounds (blue, taxifolin-CA + methyl; green, quercetin-CA + methyl). UV-spectra were recorded at 314 nm.

Neuroprotectivity in vivo

Subsequent to biological evaluation in vitro, the most active compounds taxifolin-CA and quercetin-CA were chosen for in vivo characterization in an established AD mouse model.[8b,13,23] Cognitive dysfunction was hereby induced by single intracerebroventricular injection of neurotoxic $A\beta_{25\text{-}35}$ peptide prior to treatment with the respective compound for seven days (chronic administration). The compounds were solubilised in saline using 60 % of DMSO and injected once daily intraperitoneally. Memory of the treated mice was then examined using two complementary tests, spontaneous alternation and passive avoidance, respectively. Spontaneous alternation, an index of spatial working memory, was measured in a Y-maze on day 8. Long-term memory was assessed using a step-through type passive avoidance procedure, wherein training was carried out on day 9 and retention on day 10.

Results of both experiments confirmed $A\beta_{25\text{-}35}$-induced learning impairments for both short- and long-term memory response. Regarding spontaneous alternation, taxifolin-CA and quercetin-CA attenuated learning impairments significantly at doses as low as 0.3 mg/kg (Figure 10A and C). In passive avoidance, both compounds attenuated learning impairments as well. Herein, quercetin-CA surpassed taxifolin-CA in terms of activity, showing recovery of cognitive functions at 0.3 mg/kg (Figure 10D), while taxifolin-CA is only active at 3 mg/kg (Figure 10B). In summary, both flavonoid amides attenuated $A\beta_{25\text{-}35}$ induced learning impairments. While both compounds induced recovery of spatial working memory at low doses of 0.3 mg/kg, quercetin-CA treated mice perform significantly better than taxifolin-CA regarding long-term memory.

Discussion

In this work, we describe the synthesis of flavonoid-cinnamic acid amide hybrids and their neuroprotective effect against oxytosis, ferroptosis, as well as protection against the loss of ATP, pathways highly relevant in neurodegenerative processes.[19,24] The compounds carry two pan-assay interference (PAINS) motives, a catechol and a Michael system,[25] however, the assays performed were exclusively cell-based and therefore robust against any false positive readouts.[26] The flavonoid-cinnamic acid amides form a new class of stable hybrid compounds, derived from previously published flavonoid and flavonolignan aromatic acid esters.[8] The hybridization approach has shown overadditive effects in several phenotypic screening assays related to neurodegeneration and Alzheimer's disease, exceeding the activity of the parent natural products. This led to the question, if the activity of the previously published hybrids consisting of taxifolin and cinnamic acid as esters could be improved by the exchange of taxifolin by different flavonoids, which have been proven to be more potent in phenotypic screening assays associated with neurodegeneration like fisetin[27] or eriodictyol.[28] However, this could not be observed. Overall, there is no clear trend observed when the flavone compounds are more active than the flavanones. Nevertheless, quercetin-CA was always at one concentration

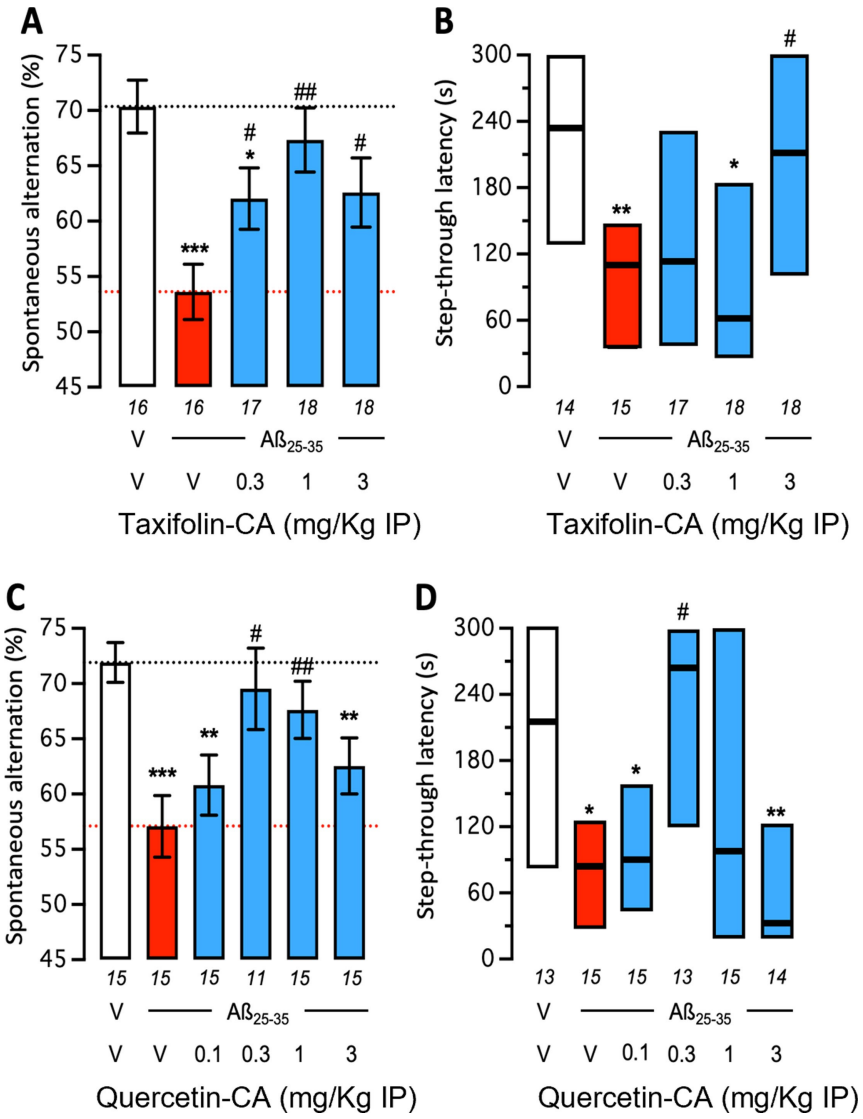

Figure 10. Effect of A, B) taxifolin-CA and C, D) quercetin-CA on A$ß_{25\text{-}35}$ induced learning impairments in mice: A, C) spontaneous alternation performance and B, D) retention latency in the passive avoidance test. Mice were treated with A$ß_{25\text{-}35}$ (9 nmol, 3 µL intracerebroventricularly) or vehicle (3 µL of ddH_2O, V1) on day 1, then received either vehicle (DMSO 60% in saline, V2), taxifolin-CA (0.3–3.0 mg/kg) or quercetin-CA (0.1–3.0 mg/kg) intraperitoneally (IP) between day 1 to 7. Mice were then tested for spontaneous alternation on day 8 and passive avoidance on day 9 (training) and day 10 (retention). Group size is shown beneath each bar graph. Data show A, C) ± SEM or median and B, D) interquartile range. ANOVA: $F_{(4,80)} = 4.997$; $p = 0.0012$ in (A); $F_{(5,80)} = 4.587$; $p = 0.0010$ in (C); Kruskal-Wallis ANOVA: $H = 12.73$; $p = 0.0127$ in (B); $H = 17.21$; $p = 0.0041$ in (D). *$p < 0.05$, **$p < 0.01$, ***$p < 0.001$ vs. V1/V2-treated group; # $p < 0.05$, ## $p < 0.01$ vs. A$ß_{25\text{-}35}$/V2 treated group; Dunnett's test in (A, C); Dunn's test in (B, D).

level lower active than the respective taxifolin hybrid. In the case of these compounds, the double bond within the C-ring has significant impact on the biological activity in vitro as well as in vivo. With the variety of assays performed, it could be shown, that the compounds act downstream the antiporter system X_c^- and downstream of the glutathione peroxidase GPx-4. The taxifolin and quercetin hybrids were tested for their influence on the production of reactive oxygen species in glutamate-induced and non-induced HT22 cells. The compounds not only prevented the formation of ROS in the oxytosis experiment (taxifolin-CA at 3.12 µM vs. quercetin-CA at 1.56 µM), but they also decreased the basal stress level in HT22 cells. Interestingly, the ROS levels were decreased in both experiments to a comparable level, at the same concentrations and with the corresponding statistical significances. This indicates that the compounds may trigger anti-oxidative pathways, which prevent formation of ROS.

Especially regarding the esters of the flavonolignan silibinin, the ester bond was hydrolysed and oxidation or disproportionation on the C-ring to the dehydro compound took place in cell culture medium.[8a,10] The esters of the flavonoid taxifolin showed a high rate of conversion to the quercetin derivative within 4 hours in cellular uptake experiments.[8b] To overcome cleavage of the ester, an amide bond had been introduced and stability measurement in cell culture medium revealed improved stability towards hydrolysis. Nevertheless, concentration

of the starting compound still decreased within 4 hours to ~55% of the starting concentration, which might be due to unspecific binding to fetal bovine serum.[29] It is known, that taxifolin aromatic acid esters get converted to the respective quercetin analogue in both RAW264.7 macrophages[8c] and BV2 microglia.[8b] Similar observations were made in this work, but the conversion of taxifolin-CA to quercetin-CA was very low compared to the previous work, which might be an indicator for a specific enzyme catalyzing this reaction, rather than an unspecific oxidation, which should lead to a similar conversion rate for all compounds. Additionally, the molecular ions of $[M+H]^+$ *m/z* 520.15 and $[M+H]^+$ *m/z* 518.15 observed, fit to methylated taxifolin-CA and quercetin-CA. The well-studied enzyme catechol-*O*-methyltransferase (COMT) is known for the methyl transfer of *S*-adenosyl methionine to catechol structures like in the neurotransmitter dopamine or other catechol-containing drugs.[30] The flavonoids quercetin and luteolin are substrates of COMT[31] suggesting that the hybrid compounds may also get methylated by COMT.

Taken together, introduction of the amide bond has led to a significant improvement of activity in vivo compared to our previous ester-based flavonoid derivatives, attenuating cognitive impairments at much lower doses. While both amides performed similarly effective in Y-maze spontaneous alternation at doses of 0.3 mg/kg, quercetin-CA could also attenuate cognitive impairments regarding long-term memory at 0.3 mg/kg, confirming our focus on stability improvement in vivo.

Conclusion

The compounds presented in this work have shown, that small changes at the flavonoid core structure go along with different biological activity profiles. Even if there was no clear trend observed regarding the influence of the double bond at the C-ring, we demonstrated, that in case of taxifolin-CA and quercetin-CA the active concentration could be reduced in vitro by introducing a double bond and even in vivo the active concentration of quercetin-CA was lower than for the respective compound without the double bond in the C-ring of the flavonoid. Taxifolin-CA showed longer occurrence in cells and was stable towards hydrolysis as expected for compounds with stable amide bonds. Interestingly, the amide compounds have shown greater activity in comparison to previous published ester compounds,[8b] indicating an important role of the amide bond. Furthermore, the two most active compounds show pronounced neuroprotectivity in vivo improving both short- and long-term memory upon chronic administration at a remarkably low dosage of 0.3 mg/kg for quercetin-cinnamic acid compound proving that the introduction of the stable amide bridge is indeed improving the compounds' properties in vivo. Further studies for a more in-depth molecular biological characterization of the mode of action of these compounds are ongoing.

Experimental Section

Chemistry

General

All reagents were used without further purification and bought from common commercial suppliers. Thin-layer chromatography was performed on silica gel 60 (alumina foils with fluorescent indicator 254 nm). UV light (254 and 366 nm) was used for detection. For column chromatography, silica gel 60 (particle size 0.040–0.063 mm) was used. Nuclear magnetic resonance (NMR) spectra were recorded with a Bruker AV-400 NMR instrument (Bruker, Karlsruhe, Germany) in $CDCl_3$ or DMSO-d_6, and chemical shifts are expressed in ppm relative to $CDCl_3$ (7.26 ppm for ^{1}H and 77.16 ppm for ^{13}C) or DMSO-d_6 (2.50 ppm for ^{1}H and 39.52 ppm for ^{13}C). Purity of the synthesis products was determined by HPLC (Shimadzu Products), containing a DGU-20 A3R degassing unit, a LC20AB liquid chromatograph, and an SPD-20 A UV/vis detector. UV detection was measured at 254 nm. Mass spectra were obtained by a LCMS 2020 (Shimadzu Products) running in positive ionisation mode. As a stationary phase, a Synergi 4 U fusion-RP (150 mm ×4.6 mm) column was used, and as a mobile phase, a gradient of methanol/water with 0.1% (v/v) formic acid. Parameters: A = water, B = methanol, V(B)/(V(A)+V(B)) = from 5% to 90% over 10 min, V(B)/(V(A)+V(B)) = 90% for 5 min, V(B)/(V(A)+V(B)) = from 90% to 5% over 3 min. The method was performed with a flow rate of 1.0 mL/min. Compounds were only used for biological evaluation if the purity was ≥95%. Melting points/decomposition (dec.) were determined using an OptiMelt automated melting point system (Scientific Instruments GmbH, Gilching, Germany).

For the preparation of the chalcones out of the respective acetophenones and aldehydes, see the Supporting Information.

Eriodictyol (2-(3,4-dihydroxyphenyl)-5,7-dihydroxychroman-4-one)

A solution of chalcone (1.20 g, 2.36 mmol) in 10% methanolic HCl (100 mL) was stirred for 60 min at reflux. The solvent was removed under reduced pressure and the crude product was purified by silica gel chromatography using an eluent of dichloromethane/methanol (10/1). The product was obtained as colourless solid in 57% yield (680 mg, 2.36 mmol). ^{1}H NMR: (400 MHz, DMSO-d_6): δ = 12.13 (s, 1H, O*H*), 9.04 (s, 2H, O*H*), 6.87 (s, 1H, Ar-*H*), 6.74 (s, 2H, Ar-*H*), 5.88–5.87 (m, 2H, Ar-*H*), 5.37 (dd, ^3J = 12.6,, ^4J = 3.1 Hz, 1H, C*H*), 3.17 (dd, ^2J = 17.1 Hz, ^3J = 12.9 Hz, 1H, C*H*) 2.68 (dd, ^2J = 17.1 Hz, ^3J = 3.1 Hz, 1H, CH) – ^{13}C NMR (100 MHz, DMSO-d_6): δ = 196.3 (C_q, *C*=O), 166.6 (C_q, Ph-*C*), 163.4 (C_q, Ph-*C*), 162.8 (C_q,Ph-*C*), 145.7 (C_q, Ph-*C*), 145.2 (C_q, Ph-*C*), 129.4 (C_q, Ph-*C*), 117.9 (+, Ph-*C*), 115.3 (+, Ph-*C*), 114.3 (+, Ph-*C*), 101.7 (C_q, Ph-*C*), 95.7 (+, Ph-*C*), 94.9 (+, Ph-*C*), 78.4 (+, *C*H), 45.6 (-, *C*H_2). – ESI-MS: $[C_{15}H_{12}O_6+H]^+$: *m/z* calcd 289.07; found 289.10 – MP 246 °C dec. Analytical data are consistent with those reported in the literature.[32]

Fustin (2-(3,4-dihydroxyphenyl)-3,7-dihydroxychroman-4-one)

A solution of chalcone (567 mg, 1.22 mmol) in 10% methanolic HCl (50 mL) was stirred for 45 min at reflux. The solvent was removed under reduced pressure and the crude product was purified by silica gel chromatography using an eluent of dichloromethane/methanol (20/1). The product was obtained as light brown solid in 57% yield (200 mg, 0.694 mmol). ^{1}H NMR: (400 MHz, DMSO-d_6): δ = 10.59 (s, 1H, O*H*), 8.98 (s, 1H, O*H*), 8.94 (s, 1H, O*H*), 7.63 (d, ^3J =

8.7 Hz, 1H, Ar-*H*), 6.88 (d, ^4J = 1.8 Hz, 1H, Ar-*H*), 6.76 (dd, ^3J = 8.2, ^4J = 1.8 Hz, 1H, Ar-*H*), 6.73 (d, ^3J = 8.0 Hz, 1H, Ar-*H*), 6.53 (dd, ^3J = 8.7, ^4J = 2.2 Hz, 1H Ar-*H*), 6.30 (d, ^4J = 2.1 Hz, 1H Ar-*H*), 5.47 (s, 1H, O*H*), 4.97 (d, ^3J = 11.3 Hz, 1H), 4.40 (dd, ^3J = 11.3, 5.2 Hz, 1H). – ^{13}C NMR (100 MHz, DMSO-d_6): δ = 192.5 (C_q, *C*=O), 164.7 (C_q, Ph-*C*), 162.7 (C_q,Ph-*C*), 145.6 (C_q, Ph-*C*), 144.8 (C_q, Ph-*C*), 128.6 (C_q, Ph-*C*), 128.3 (+, Ph-*C*), 119.4 (+, Ph-*C*), 115.3 (+, Ph-*C*), 115.0 (+, Ph-*C*), 112.1 (C_q, Ph-*C*), 110.5 (+, Ph-*C*), 102.3 (+, Ph-*C*), 83.5 (+, *C*H), 72.5 (+, *C*H). – ESI-MS: $[C_{15}H_{12}O_6+H]^+$: *m/z* calcd 289.07; found 289.11 – MP 205 °C dec. The analytical data are consistent with those reported in the literature.[33]

General Procedure for acetyl protection of flavonoids

To a suspension of the respective flavonoid (1 equiv.) in acetic anhydride (10 equiv.), iodine (0.07 equiv.) was added, and the reaction mixture was stirred 2 h at room temperature. For protected flavanones, ethyl acetate was added, and the mixture was washed with saturated $Na_2S_2O_3$-solution (aq.) and saturated $NaHCO_3$-solution (aq.). The organic layer was dried over Na_2SO_4, and the solvent was removed under reduced pressure. The crude products were recrystallized in a mixture of cyclohexane and ethyl acetate (1/1) and the products were obtained as colourless solid.

For protected quercetin and fisetin, the precipitant was filtered off and washed with cyclohexane, saturated $Na_2S_2O_3$-solution (aq.) and saturated $NaHCO_3$-solution (aq.). The residues were dissolved in dichloromethane and washed with saturated $NaHCO_3$-solution (aq.) and brine. The organic layer was dried over Na_2SO_4, and the solvent was removed under reduced pressure. The products were obtained as colourless solid.

Penta-O-acetyl taxifolin (2-(3,4-diacetoxyphenyl)-4-oxochromane-3,5,7-triyl triacetate)

Yield: 77% – ^{1}H NMR: (400 MHz, $CDCl_3$): δ = 7.37 (dd, ^3J = 8.4, ^4J = 2.1 Hz, 1H, Ph), 7.28 (d, ^4J = 2.1 Hz, 1H, Ph), 7.25 (d, ^3J = 8.4, 1H, Ph), 6.77 (d, ^4J = 2.3, 1H), 6.59 (d, ^4J = 2.2, 1H), 5.64 (d, ^3J = 12.3 Hz, 1H), 5.41 (d, ^3J = 12.3 Hz, 1H), 2.36 (s, 3H, OAc), 2.28 (s, 6H, OAc), 2.20 (s, 3H, OAc), 2.03 (s, 3H, OAc). – ^{13}C NMR (100 MHz, $CDCl_3$): δ = 184.8 (C_q, *C*=O), 169.2 (C_q, CH_3*C*OO), 169.1 (C_q, CH_3*C*OO), 168.0 (C_q, CH_3*C*OO), 168.0 (C_q, CH_3*C*OO), 167.9 (C_q, CH_3*C*OO), 162.4 (C_q, Ph), 156.4 (C_q, Ph), 151.4 (C_q, Ph), 143.0 (C_q, Ph), 142.2 (C_q, Ph), 133.5 (C_q, Ph-*C*), 125.3 (+, Ph-*C*), 123.8 (+, Ph-*C*), 122.8 +, Ph-*C*), 111.4 (+, Ph-*C*), 110.6 (C_q, Ph-*C*), 109.0 (+, Ph-*C*), 80.3 (+, *C*H), 73.1 (+, *C*H), 22.1 (+, CH_3*C*OO), 20.9 (+, CH_3*C*OO), 20.6 (+, CH_3*C*OO), 20.6 (+, CH_3*C*OO), 20.2 (+, CH_3*C*OO). – ESI-MS $[C_{25}H_{22}O_{12}+Na]^+$: *m/z* calcd 537.12; found 537.10. – MP 145 °C. Analytical data are consistent with those reported in the literature.[34]

Penta-O-acetyl quercetin (2-(3,4-diacetoxyphenyl)-4-oxo-4H-chromene-3,5,7-triyl triacetate)

Yield: 75% – ^{1}H NMR: (400 MHz, $CDCl_3$): δ = 7.71 (dd, ^3J = 8.4, ^4J = 2.1 Hz, 1H, Ph), 7.69 (d, ^4J = 2.1 Hz, 1H, Ph), 7.35 (d, ^3J = 8.5, 1H, Ph), 7.33 (d, ^4J = 2.2 Hz, 1H, Ph), 6.87 (d, ^4J = 2.2, 1H, Ph), 2.43 (s, 3H, CH_3*C*OO), 2.33 (s, 6H, CH_3*C*OO), 2.32 (s, 6H, CH_3*C*OO). – ^{13}C NMR (100 MHz, $CDCl_3$): δ = 170.2 (C_q, *C*=O), 169.3 (C_q, CH_3*C*OO), 168.0 (C_q, CH_3*C*OO), 167.9 (C_q, CH_3*C*OO), 167.9 (C_q, CH_3*C*OO), 167.8 (C_q, CH_3*C*OO), 157.0 (C_q, Ph-*C*), 154.4 (C_q, 2×Ph-*C*), 153.9 (C_q, Ph-*C*), 150.5 (C_q, Ph-*C*), 144.5 (C_q, Ph-*C*), 142.3 (C_q, Ph-*C*), 134.2 (C_q, Ph-*C*), 127.8 (+, Ph-*C*), 124.0 (+, Ph-*C*), 123.9 (+, Ph-*C*), 114.9 (+, Ph-*C*), 114.0 (+, Ph-*C*), 109.1 (+, Ph-*C*), 21.3 (+, CH_3*C*OO), 21.2 (+, CH_3*C*OO), 20.7 (+, 2×CH_3*C*OO), 20.6 (+, CH_3*C*OO). – ESI-MS $[C_{25}H_{21}O_{12}+H]^+$: *m/z* calcd 513.10; found 513.20 – MP 191 °C. Analytical data are consistent with those reported in the literature.[11]

Tetra-O-acetyl eriodictyol (4-(5,7-diacetoxy-4-oxochroman-2-yl)-1,2-phenylene diacetate)

Yield: 83% – ^{1}H NMR: (400 MHz, $CDCl_3$): δ = 7.35–7.29 (m, 2H, Ar–H), 7.25 (d, ^3J = 8.8 Hz, 1H, Ar–H), 6.79 (d, ^4J = 2.2, 1H), 6.55 (d, ^4J = 2.2 Hz, 1H), 5.48 (dd, ^3J = 13.6, ^4J = 2.8 Hz, 1H), 3.00 (dd, ^2J = 16.7 Hz, ^3J = 13.6 Hz, 1H), 2.80 (dd, ^2J = 16.7, ^3J = 13.6 Hz, 1H), 2.38 (s, 3H, OAc), 2.31 (s, 3H, OAc), 2.30 (s, 3H, OAc), 2.30 (s, 3H, OAc). – ^{13}C NMR (100 MHz, $CDCl_3$): δ = 188.7 (C_q, *C*=O), 169.4 (C_q, CH_3*C*OO), 168.2 (C_q, CH_3*C*OO), 168.1 (C_q, CH_3*C*OO), 168.0 (C_q, CH_3*C*OO), 163.0 (C_q, Ph-*C*), 156.1 (C_q, Ph-*C*), 151.4 (C_q, CH_3*C*OO) 142.5 (C_q, 2×Ph), 137.0 (C_q, Ph-*C*), 124.3 (+, Ph-*C*), 124.0 (+, Ph-*C*), 121.5 (+, Ph-*C*), 111.9 (C_q, Ph-*C*), 110.0 (+, Ph-*C*), 109.2 (+, Ph-*C*), 78.6 (+, *C*H), 60.5 (-, CH_2), 21.3 (+, CH_3COO), 21.1 (+, CH_3COO), 20.8 (+, CH_3COO) 20.7 (+, CH_3COO). – ESI-MS $[C_{23}H_{21}O_{10}+H]^+$: *m/z* calcd 457.11; found 457.15. – MP 133 °C. Analytical data are consistent with those reported in the literature.[35]

Tetra-O-acetyl luteolin (4-(5,7-diacetoxy-4-oxo-4H-chromen-2-yl)-1,2-phenylene diacetate)

Dibenzoyl peroxide (12 mg, 0.05 mmol) was added to a solution of tetra-*O*-eriodictyol (233 mg, 0.511 mmol) and *N*-bromosuccinimide (109 mg, 0.613 mmol) in chloroform (2.5 mL) and heated to reflux for 2 h. Chloroform was added (25 mL) and the mixture was washed with water (50 mL) and brine (25 mL). The organic layer was dried over Na_2SO_4, and the solvent was removed under reduced pressure. The crude product was purified by silica gel column chromatography using an eluent of cyclohexane and ethyl acetate (2/1 → pure ethyl acetate). The product was obtained as colourless solid in 60% yield (139 mg, 0.306 mmol). ^{1}H NMR: (400 MHz, $CDCl_3$): δ = 7.72 (dd, ^3J = 8.5, ^4J = 2.3 Hz, 1H, Ph), 7.69 (d, ^4J = 2.1 Hz, 1H, Ph), 7.35 (d, ^3J = 8.5, 1H, Ph), 7.33 (d, ^4J = 2.2 Hz, 1H, Ph), 6.85 (d, ^4J = 2.2, 1H, Ph), 6.60 (s, 1H, C=*CH*), 2.43 (s, 3H, CH_3*C*OO), 2.33 (s, 6H, CH_3*C*OO), 2.31 (s, 3H, CH_3*C*OO). – ^{13}C NMR (100 MHz, $CDCl_3$): δ = 176.2 (C_q, *C*=O), 169.4 (C_q, CH_3*C*OO), 168.0 (C_q, 2×CH_3*C*OO), 167.8 (C_q, CH_3*C*OO), 160.8 (C_q, Ph-*C*), 157.6 (C_q, Ph-*C*), 154.1 (C_q, Ph-*C*), 150.3 (C_q, Ph-*C*), 144.9 (C_q, Ph-*C*), 142.7 (C_q, Ph-*C*), 129.7 (C_q, Ph-*C*), 124.6 (+, Ph-*C*), 124.4 (+, Ph-*C*), 121.7 (+, Ph-*C*), 115.0 (C_q, Ph-*C*), 113.9 (+, Ph-*C*), 109.1 (+, Ph-*C*), 109.0 (+, C=*CH*), 21.3 (+, CH_3*C*OO), 21.1 (+, CH_3*C*OO), 20.8 (+, CH_3*C*OO), 20.7 (+, CH_3*C*OO). – ESI-MS $[C_{23}H_{19}O_{10}+H]^+$: *m/z* calcd 455.10; found 455.15 – MP 213 °C. Analytical data are consistent with those reported in the literature.[36]

Tetra-O-acetyl fustin (4-(3,7-diacetoxy-4-oxochroman-2-yl)-1,2-phenylene diacetate)

Yield: 67% – ^{1}H NMR: (400 MHz, $CDCl_3$): δ = 7.94 (d, ^3J = 8.6 Hz, 1H, Ar–H), 7.41 (dd, ^3J = 8.4, ^4J = 2.1 Hz, 1H, Ar–H), 7.32 (d, ^4J = 2.1 Hz, 1H, Ar–H), 7.27 (d, ^3J = 8.7, 1H, Ar–H), 6.87 (dd, ^3J = 8.6, ^4J = 2.1, 1H), 6.84 (d, ^4J = 2.1, 1H), 5.72 (d, ^3J = 12.2 Hz, 1H), 5.44 (d, ^3J = 12.2 Hz, 1H), 2.31 (s, 3H, OAc), 2.30 (s, 6H, OAc), 2.07 (s, 3H, OAc). – ^{13}C NMR (100 MHz, $CDCl_3$): δ = 187.1 (C_q, *C*=O), 169.3 (C_q, CH_3*C*OO), 168.4 (C_q, CH_3*C*OO), 168.1 (C_q, CH_3*C*OO), 168.0 (C_q, CH_3*C*OO), 161.7 (C_q, Ph-*C*), 157.1 (C_q, Ph-*C*), 142.9 (C_q, Ph), 142.2 (C_q,Ph), 133.9 (C_q, Ph-*C*), 129.1 (+, Ph-*C*), 125.4 (+, Ph-*C*), 123.9 (+, Ph-*C*), 122.9 (+, Ph-*C*), 117.6 (C_q, Ph-*C*), 116.7 (+, Ph-*C*), 111.2 (+, Ph-*C*), 81.0 (+, *C*H), 73.7 (+, *C*H), 21.2 (+, CH_3*C*OO), 20.8 (+, CH_3*C*OO), 20.6 (+, CH_3*C*OO) 20.4 (+, CH_3*C*OO). – ESI-MS $[C_{23}H_{21}O_{10}+H]^+$: *m/z* calcd 457.11; found 457.10. – MP 138 °C.

Tetra-O-acetyl fisetin (4-(3,7-diacetoxy-4-oxo-4H-chromen-2-yl)-1,2-phenylene diacetate)

Yield: 84% – ^{1}H NMR: (400 MHz, $CDCl_3$): δ = 8.25 (d, ^3J = 8.8 Hz, 1H, Ph), 7.77-7.74 (m, 2H, Ph), 7.40 (d, ^4J = 2.1, 1H, Ph), 7.36 (d, ^3J = 8.3 Hz, 1H, Ph), 7.18 (dd, ^{3}J = 8.9 Hz, ^{4}J = 1.74 Hz, 1H, Ph), 2.36 (s, 3H, CH_3COO), 2.35 (s, 3H, CH_3COO), 2.33 (s, 6H, CH_3COO). – ^{13}C NMR (100 MHz, $CDCl_3$): δ = 171.6 (C_q, *C*=O), 168.5 (C_q, CH_3COO), 168.1 (C_q, CH_3COO), 167.9 (C_q, CH_3COO), 167.9 (C_q, CH_3COO), 156.0 (C_q, Ph-*C*), 155.0 (C_q, Ph-*C*), 154.9 (C_q, Ph-*C*), 144.5 (C_q, Ph-*C*), 142.3 (C_q, Ph-*C*), 134.0 (C_q, Ph-*C*), 128.2 (C_q, Ph-*C*), 127.6 (+, Ph-*C*), 126.6 (C_q, Ph-*C*), 124.1 (+, Ph-*C*), 124.0 (+, Ph-*C*), 121.4 (+, Ph-*C*), 119.8 (+, Ph-*C*), 111.1 (+, Ph-*C*), 21.3 (+, CH_3COO), 20.8 (+, 2×CH_3COO), 20.6 (+, CH_3COO). – ESI-MS $[C_{23}H_{18}O_{10}+Na]^+$: *m/z* calcd 455.10; found 455.15 – MP 197 °C.

General procedure for deprotection of the position 7

The selective deprotection was done like previously described.[11] A solution of imidazole (2.00 equiv.) in dichloromethane was added dropwise to an −15 °C cold solution of the respective peracetylted flavonoid in dichloromethane. The reaction mixture was warmed to room temperature and stirred for 2 hours. Dichloromethane was added and the solution was washed with 5% HCl and brine. The organic layer was dried over Na_2SO_4, and the solvent was removed under reduced pressure. The crude product was purified by silica gel chromatography using an eluent of dichloromethane/methanol (40/1). The products were obtained as colourless foam.

7-OH-Taxifolin (4-(3,5-diacetoxy-7-hydroxy-4-oxochroman-2-yl)-1,2-phenylene diacetate)

Yield: 40% – ^{1}H NMR: (400 MHz, $CDCl_3$): δ = 7.31 (dd, ^3J = 8.4, ^4J = 2.1 Hz, 1H, Ph), 7.25 (d, ^4J = 2.1 Hz, 1H), 7.23 (d, ^3J = 8.3 Hz, 1H, Ph), 6.19 (d, ^4J = 2.3, 1H, Ph), 6.11 (d, ^4J = 2.3, 1H, Ph) 5.58 (d, ^3J = 12.1 Hz, 1H), 5.30 (d, ^3J = 12.2 Hz, 1H), 2.37 (s, 3H, CH_3COO), 2.31 (s, 3H, CH_3COO), 2.30 (s, 3H, CH_3COO), 2.00 (s, 3H, CH_3COO). – ^{13}C NMR (100 MHz, $CDCl_3$): δ = 185.8 (C_q, *C*=O), 170.7 (C_q, CH_3COO), 169.6 (C_q, CH_3COO), 168.7 (C_q, CH_3COO), 168.6 (C_q, CH_3COO), 164.0 (C_q, Ph-*C*), 163.2 (C_q, Ph-*C*), 152.0 (C_q, Ph-*C*), 142.8 (C_q, Ph-*C*), 142.1 (C_q, Ph-*C*), 134.2 (C_q, Ph-*C*), 125.7 (+, Ph-*C*), 123.9 (+, Ph-*C*), 122.9 (+, Ph-*C*), 111.4 (C_q, Ph-*C*), 106.5 (+, Ph-*C*), 102.0 (+, Ph-*C*), 80.2 (+, *C*H), 73.1 (+, *C*H), 21.2 (+, CH_3COO), 20.7 (+, 2×CH_3COO), 20.5 (+, CH_3COO). – ESI-MS $[C_{23}H_{20}O_{11}+H]^+$: *m/z* calcd 473.11; found 473.05. MP 134 °C. Analytical data are consistent with those reported in the literature.[37]

7-OH-Quercetin (4-(3,5-diacetoxy-7-hydroxy-4-oxo-4H-chromen-2-yl)-1,2-phenylene diacetate)

Yield: 48% – ^{1}H NMR: (400 MHz, $CDCl_3$): δ = 7.66-7.64 (m, 2H, Ph), 7.29 (d, ^{3}J = 9.1 Hz, 1H, Ph), 6.63 (d, ^4J = 2.3 Hz, 1H, Ph), 6.50 (d, ^4J = 2.3 Hz, 1H, Ph), 2.38 (s, 3H, CH_3COO), 2.32 (s, 3H, CH_3COO), 2.31 (s, 6H, CH_3COO). – ^{13}C NMR (100 MHz, $CDCl_3$): δ = 170.7 (C_q, *C*=O), 170.2 (C_q, CH_3COO), 168.8 (C_q, CH_3COO), 168.2 (C_q, CH_3COO), 168.1 (C_q, CH_3COO), 162.1 (C_q, Ph-*C*), 158.0 (C_q, Ph-*C*), 153.6 (C_q, Ph-*C*), 150.7 (C_q, Ph-*C*), 144.4 (C_q, Ph-*C*), 142.2 (C_q, Ph-*C*), 133.4 (C_q, Ph-*C*), 128.0 (C_q, Ph-*C*), 126.6 (+, Ph-*C*), 124.0 (+, Ph-*C*), 123.8 (+, Ph-*C*), 110.3 (C_q, Ph-*C*), 109.7 (+, Ph-*C*), 101.3 (+, Ph-*C*), 21.2 (+, CH_3COO), 20.8 (+, 2×CH_3COO), 20.7 (+, CH_3COO). – ESI-MS $[C_{23}H_{18}O_{11}+H]^+$: *m/z* calcd 471.08; found 471.10. MP 180 °C. Analytical data are consistent with those reported in the literature.[11]

7-OH-Eriodictyol (4-(5-acetoxy-7-hydroxy-4-oxochroman-2-yl)-1,2-phenylene diacetate)

Yield: 45% – ^{1}H NMR: (400 MHz, $CDCl_3$): δ = 7.32 (d, ^{4}J = 1.6 Hz, 1H, Ar–H), 7.26 (d, ^{3}J = 1.1 Hz, 2H, Ar–H), 6.20 (d, ^4J = 2.3, 1H), 6.16 (d, ^4J = 2.4 Hz, 1H), 5.35 (dd, ^3J = 13.4, ^{4}J = 2.8 Hz, 1H), 2.93 (dd, ^2J = 16.7 Hz, ^{3}J = 13.5 Hz, 1H), 2.72 (dd, ^2J = 16.7, ^{3}J = 2.9 Hz, 1H), 2.43 (s, 3H, OAc), 2.36 (s, 3H, OAc), 2.36 (s, 3H, OAc). – ^{13}C NMR (100 MHz, $CDCl_3$): δ = 188.7 (C_q, *C*=O), 170.6 (C_q, CH_3COO), 168.7 (C_q, CH_3COO), 168.5 (C_q, CH_3COO), 163.9 (C_q, Ph-*C*), 163.3 (C_q, Ph-*C*), 151.9 (C_q, CH_3COO), 142.3 (C_q, Ph-*C*), 142.2 (C_q, Ph-*C*), 137.4 (C_q, Ph-*C*), 124.7 (+, Ph-*C*), 124.0 (+, Ph-*C*), 121.6 (+, Ph-*C*), 107.5 (C_q, Ph-*C*), 105.8 (+, Ph-*C*), 102.0 (+, Ph-*C*), 78.4 (+, *C*H), 44.7 (-, CH_2), 21.3 (+, CH_3COO), 20.7 (+, 2×CH_3COO). – ESI-MS $[C_{21}H_{18}O_9+H]^+$: *m/z* calcd 415.10; found 415.15. – MP 128 °C.

7-OH-Luteolin (4-(5-acetoxy-7-hydroxy-4-oxo-4H-chromen-2-yl)-1,2-phenylene diacetate)

Yield: 31% – ^{1}H NMR: (400 MHz, DMSO-d_6): δ = 11.15 (s, 1H, O*H*), 8.00-7.98 (m, 2H, Ar-*H*), 7.48 (d, ^{3}J = 9.2 Hz, 1H, Ar-*H*), 6.95 (d, ^{4}J = 2.3 Hz, 1H, Ar-*H*), 6.77 (s, 1H, C=*CH*), 6.57 (d, ^{4}J = 2.3 Hz, 1H, Ar-*H*), 2.33 (s, 3H, CH_3COO), 2.31 (s, 6H, CH_3COO), 2.29 (s, 3H, CH_3COO). – ^{13}C NMR (100 MHz, DMSO-d_6): δ = 175.1 (C_q, *C*=O), 168.8 (C_q, CH_3COO), 168.2 (C_q, CH_3COO), 167.9 (C_q, CH_3COO), 162.3 (C_q, Ph-*C*), 159.4 (C_q, Ph-*C*), 158.2 (C_q, Ph-*C*), 150.0 (C_q, Ph-*C*), 144.5 (C_q, Ph-*C*), 142.5 (C_q, Ph-*C*), 129.4 (C_q, Ph-*C*), 124.7 (+, Ph-*C*), 124.5 (+, Ph-*C*), 121.7 (+, Ph-*C*), 109.4 (C_q, Ph-*C*), 108.8 (+, Ph-*C*), 107.9 (+, Ph-*C*), 100.9 (+, C=*C*H), 20.9 (+, CH_3COO), 20.4 (+, CH_3COO), 20.3 (+, CH_3COO). – ESI-MS $[C_{23}H_{19}O_{10}+H]^+$: *m/z* calcd 413.09; found 413.20 – MP 191 °C. The analytical data are consistent with those reported in the literature.[36b]

7-OH-Fustin (4-(3-acetoxy-7-hydroxy-4-oxochroman-2-yl)-1,2-phenylene diacetate)

Yield: 44% – ^{1}H NMR: (400 MHz, $CDCl_3$): δ = 7.80 (d, ^{3}J = 8.6 Hz, 1H, Ar–H), 7.40 (dd, ^3J = 8.4, ^4J = 2.1 Hz, 1H, Ar–H), 7.31 (d, ^4J = 2.1 Hz, 1H, Ar–H), 7.25 (d, ^3J = 8.6, 1H, Ar–H), 6.53 (dd, ^{3}J = 8.7, ^4J = 2.3, 1H), 6.41 (d, ^4J = 2.2, 1H), 5.67 (d, ^3J = 12.2 Hz, 1H), 5.37 (d, ^3J = 12.1 Hz, 1H), 2.31 (s, 3H, OAc), 2.30 (s, 3H, OAc), 2.07 (s, 3H, OAc). – ^{13}C NMR (100 MHz, $CDCl_3$): δ = 186.8 (C_q, *C*=O), 169.7 (C_q, CH_3COO), 168.3 (C_q, CH_3COO), 168.3 (C_q, CH_3COO), 163.7 (C_q, 2×Ph-*C*), 142.8 (C_q, Ph), 142.2 (C_q, Ph), 134.4 (C_q, Ph-*C*), 129.9 (+, Ph-*C*), 125.5 (+, Ph-*C*), 123.9 (+, Ph-*C*), 122.9 (+, Ph-*C*), 113.5 (C_q, Ph-*C*), 111.7 (+, Ph-*C*), 103.5 (+, Ph-*C*), 80.8 (+, *C*H), 73.8 (+, *C*H), 20.8 (+, CH_3COO), 20.7 (+, CH_3COO), 20.5 (+, CH_3COO). – ESI-MS $[C_{21}H_{18}O_9+H]^+$: *m/z* calcd 415.11; found 415.15. – MP 143 °C.

7-OH-Fisetin (4-(3-acetoxy-7-hydroxy-4-oxo-4H-chromen-2-yl)-1,2-phenylene diacetate)

Yield: 30% – ^{1}H NMR: (400 MHz, $CDCl_3$): δ = 8.26 (d, ^{3}J = 8.7, 1H, Ph), 7.72 (d, ^{4}J = 2.1 Hz, 1H, Ph), 7.69 (dd, ^{3}J = 8.5, ^4J = 2.2 Hz, 1H, Ph), 7.40 (d, ^{3}J = 2.1 Hz, 1H, Ph), 7.17 (dd, ^{3}J = 8.7, ^{4}J = 2.1 Hz, 1H, Ph), 7.13 (d, ^{3}J = 8.5 Hz, 1H, Ph), 2.41 (s, 3H, CH_3COO), 2.37 (s, 3H, CH_3COO), 2.36 (s, 3H, CH_3COO). – ^{13}C NMR (100 MHz, $CDCl_3$): δ = 170.2 (C_q, *C*=O), 168.2 (C_q, CH_3COO), 168.0 (C_q, CH_3COO), 167.9 (C_q, CH_3COO), 156.9 (C_q, Ph-*C*), 153.1 (C_q, Ph-*C*), 152.4 (C_q, Ph-*C*), 144.1 (C_q, Ph-*C*), 142.1 (C_q, Ph-*C*), 132.8 (C_q, Ph-*C*), 127.8 (C_q, Ph-*C*), 127.4 (+, Ph-*C*), 126.5 (C_q, Ph-*C*), 126.9 (+, Ph-*C*), 124.9 (+, Ph-*C*), 124.0 (+

, Ph-*C*), 116.1 (+, Ph-*C*), 103.1 (+, Ph-*C*), 20.8 (+, CH_3COO), 20.7 (+, CH_3COO), 20.6 (+, CH_3COO). – ESI-MS $[C_{21}H_{16}O_9+H]^+$: *m/z* calcd 413.36; found 413.30 – MP 213 °C.

N-(4-Bromobutyl)cinnamamide

To an ice-cold solution of cinnamic acid (174 mg, 1.17 mmol) and DMF (10 µL) in dry dichloromethane (10 mL) oxychloride (149 µL, 1.29 mmol) was added. The solution was stirred 1 h at room temperature before 4-bromobutan-1-amonie hydrobromide (300 mg, 1.29 mmol) was added. A solution of NEt_3 (734 µL, 5.27 mmol.) in dry dichloromethane (5 mL) was added and the reaction mixture was stirred 1 h. Water (30 mL) was added, and the mixture was extracted with dichloromethane (90 mL). The combined organic layers were washed with 5% HCl-solution (150 mL), saturated $NaHCO_3$-solution (100 mL) and brine (50 mL) and dried over Na_2SO_4. The solvent was removed under reduced pressure and the product was obtained as pale-yellow solid in 80% yield (287 mg).

^{1}H NMR: (400 MHz, $CDCl_3$): δ = 7.62 (d, $^3J_{trans}$ = 15.6 Hz, 1H), 7.48 (m, 2H, Ph), 7.35 (m, 3H, Ph), 6.41 (d, $^3J_{trans}$ = 15.6 Hz, 1H), 5.90 (s, 1H, N*H*), 3.43 (m, 4H, CH_2), 1.99 – 1.88 (m, 2H, CH_2), 1.79 – 1.70 (m, 2H, CH_2). – ^{13}C NMR (100 MHz, $CDCl_3$): δ = 166.2 (C_q, C = CONH), 141.2 (+, HC=CH), 134.9 (C_q, Ph), 129.8 (+, Ph-*C*), 128.9 (+, 2×Ph-*C*), 127.8 (+, 2×Ph-*C*), 120.7 (+, HC=CH), 38.9 (CH_2), 33.4 (CH_2), 30.1 (CH_2), 28.4 (CH_2). – ESI-MS $[C_{13}H_{16}BrNO+H]^+$: *m/z* calcd 282.05; found 282.10. – MP 101 °C.

N-(4-Iodobutyl)cinnamamide

A suspension of NaI (800 mg, 5.33 mol) and N-(4-bromobutyl)cinnamamide (287 mg, 1.07 mmol) in dry acetone (10 mL) was heated to reflux for 1.5 h. The solution was diluted with water (20 mL) and extracted with ethyl acetate (80 mL). The organic layer was washed with water (50 mL) and brine (50 mL) and dried over Na_2SO_4. The solvent was removed under reduced pressure and the crude product was used directly without further purification.

General procedure for ether synthesis and deprotection

N-(4-iodobutyl)cinnamamide (1.2 equiv.) and K_2CO_3 (1 equiv.) were added to a solution of the respective 7-*OH*-flavonoid in dry DMF under argon atmosphere and stirred overnight (16 h) at room temperature. Dichloromethane was added and the organic layer was washed with 5% $HCl_{(aq.)}$ and brine. The organic layer was dried over Na_2SO_4, and the solvent was removed under reduced pressure. The crude product was dissolved in acetonitrile and the same amount of concentrated $HCl_{(aq.)}$ was added. The reaction mixture was stirred 15 minutes at 70 °C. Ethyl acetate was added, and the organic layer was washed with 5% $HCl_{(aq.)}$ and brine. The organic layer was dried over Na_2SO_4, and the solvent was removed under reduced pressure. The crude product was purified using an Interchim Puri Flash 430 purification system equipped with a 12 g C18 50 µm spherical RP column as stationary phase. A mixture of A = water, B = methanol was used a mobile phase, V(B)/(V(A) + V(B)) = from 10% to 70% over 15 min, V(B)/(V(A) + V(B)) = 70% for 35 min. The method was performed with a flow rate of 30.0 mL/min.

Taxifolin-cinnamic acid amide (N-(4-((2-(3,4-dihydroxyphenyl)-3,5-dihydroxy-4-oxochroman-7-yl)oxy)butyl)cinnamamide)

The product was obtained as colourless solid in 15% yield (40 mg).

^{1}H NMR: (400 MHz, DMSO-d_6): δ = 11.46 (s, 1H, O*H*), 9.08 (s, 2H, O*H*), 8.12 (t, ^3J = 5.7 Hz, 1H, N*H*), 7.54 (d, ^{3}J = 7.27 Hz, 2H, Ar-*H*), 7.42–7.34 (m, 4H, 3×Ar-*H*, *HC*=CH), 6.89 (s, 1H, Ar-*H*), 6.75 (s, 2H, Ar-*H*), 6.61 (d, $^3J_{trans}$ = 15.8 Hz, 1H, HC=*CH*), 6.10 (d, ^4J = 2.2 Hz, 1H, Ar-*H*), 6.07 (d, ^4J = 2.2 Hz, 1H), 5.78 (s, 1H, *OH*), 5.02 (d, ^3J = 11.2 Hz, 1H, O*CH*), 4.54 (d, ^3J = 11.3 Hz, 1H, *CH*), 4.05 (t, ^3J = 6.3 Hz, 2H, OCH_2), 3.22 (q, ^3J = 6.6 Hz, 2H, N*CH*), 1.72 (m, 2H, CH_2), 1.58 (m, 2H, CH_2) ppm. – ^{13}C NMR (100 MHz, DMSO-d_6): δ 198.2 (C_q, *C* = O), 166.9 (C_q, Ar-*C*), 164.8 (N*C* = O), 162.9 (C_q, Ar-*C*), 162.4 (C_q, Ar-*C*), 145.7 (C_q, Ar-*C*), 144.9 (C_q, Ar-*C*), 138.4 (+, HC = CH), 134.9 (C_q, Ar-*C*), 129.3 (+, Ar-*C*), 128.9 (+, 2×Ar-*C*), 127.8 (C_q, Ar-*C*), 127.4 (+, 2×Ar-*C*), 122.2 (+, HC = CH), 119.3 (+, Ar-*C*), 115.3 (+, Ar-*C*), 115.0 (+, Ar-*C*), 101.3 (C_q, Ar-*C*), 95.2 (+, Ar-*C*), 94.1 (+, Ar-*C*), 83.1 (+, *CH*), 71.6 (+, *CH*), 68.0 (-, OCH_2), 38.2 (-, NCH_2), 25.9 (-, CH_2), 25.6 (-, CH_2) ppm. – ESI-MS $[C_{28}H_{27}NO_8+H]^+$: *m/z* calcd 506.18; found 506.15. – MP 153 °C dec.

Quercetin-cinnamic acid amide (N-(4-((2-(3,4-dihydroxyphenyl)-3,5-dihydroxy-4-oxo-4H-chromen-7-yl)oxy)butyl)cinnamamide)

The product was obtained as yellow solid in yield 10% (15 mg).

^{1}H NMR: (400 MHz, DMSO-d_6): δ = 12.46 (s, 1H, O*H*), 9.44 (s, 2H, O*H*), 8.15 (t, ^3J = 5.8 Hz, 1H, N*H*), 7.73 (d, ^{4}J = 1.85 Hz, 1H, Ar-*H*), 7.58–7.53 (m, 3H, 3×Ar-*H*), 7.45–7.34 (m, 4H, 3×Ar-*H*, *HC*=CH), 6.89 (d, 1H, ^3J = 8.4 Hz, Ar-*H*), 6.70 (dd, 1H, ^{3}J = 8.05, ^{4}J = 2.2 Hz, Ar-*H*), 6.62 (d, $^3J_{trans}$ = 15.8 Hz, 1H, HC=*CH*), 6.33 (d, ^4J = 2.2 Hz, 1H, Ar-*H*), 4.12 (t, ^3J = 5.1 Hz, 2H, OCH_2), 3.26 (q, ^3J = 6.5 Hz, 2H, N*CH*), 1.73 (m, 2H, CH_2), 1.62 (m, 2H, CH_2) ppm. – ^{13}C NMR (100 MHz, DMSO-d_6): δ 175.9 (C_q, *C* = O), 164.9 (N*C* = O), 164.2 (C_q, Ar-*C*), 160.3 (C_q, Ar-*C*), 156.0 (C_q, Ar-*C*), 147.8 (C_q, Ar-*C*), 147.2 (C_q, Ar-*C*), 145.0 (C_q, Ar-*C*), 138.4 (+, HC = CH), 136.0 (C_q, Ar-*C*), 134.9 (C_q, Ar-*C*), 129.3 (+, Ar-*C*), 128.9 (+, 2×Ar-*C*), 127.4 (+, 2×Ar-*C*), 122.3 (+, HC = CH), 121.84 (C_q, Ar-*C*), 119.9 (+, Ar-*C*), 115.5 (+, Ar-*C*), 115.2 (+, Ar-*C*), 103.9 (C_q, Ar-*C*), 97.4 (+, Ar-*C*), 92.2 (+, Ar-*C*), 68.1 (-, OCH_2), 38.2 (-, NCH_2), 26.0 (-, CH_2), 25.7 (-, CH_2) ppm. – ESI-MS $[C_{28}H_{25}NO_8+H]^+$: *m/z* calcd 504.16; found 504.15. – MP 205 °C dec.

Eriodictyol-cinnamic acid amide (N-(4-((2-(3,4-dihydroxyphenyl)-5-hydroxy-4-oxochroman-7-yl)oxy)butyl)cinnamamide)

The product was obtained as colourless solid in 55% yield (31 mg).

^{1}H NMR: (400 MHz, DMSO-d_6): δ = 12.10 (s, 1H, O*H*), 9.04 (s, 2H, O*H*), 8.13 (t, ^3J = 5.7 Hz, 1H, N*H*), 7.58–7.51 (m, 2H, Ar-*H*), 7.45–7.34 (m, 4H, Ar-*H*), 6.89 (d, ^4J = 1.3 Hz, 1H, Ar-*H*), 6.75 (d, ^4J = 1.2 Hz, 2H, Ar-*H*), 6.62 (d, $^3J_{trans}$ = 15.8 Hz, 1H, HC=*CH*), 6.08 (d, ^4J = 2.3 Hz, 1H, Ar-*H*), 6.07 (d, ^4J = 2.3 Hz, 1H, Ar-*H*), 5.41 (dd, $^3J_{trans}$ = 12.5, $^3J_{cis}$ = 3.0 Hz, 1H, O*CH*), 4.05 (t, ^3J = 6.4 Hz, 2H, OCH_2), 3.27 – 3.17 (m, 3H, CH_2, *CH*), 2.71 (dd, ^2J = 17.2, $^3J_{cis}$ = 3.1 Hz, 1H, *CH*), 1.73 (m, 2H, CH_2), 1.58 (m, 2H, CH_2). ppm. – ^{13}C NMR (100 MHz, DMSO-d_6): δ 196.28(C_q, *C* = O), 166.7 (C_q, Ar-*C*), 164.8 (N*C* = O), 163.1 (C_q, Ar-*C*), 162.8 (C_q, Ar-*C*), 145.8 (C_q, Ar-*C*), 145.2 (C_q, Ar-*C*), 138.5 (+, H*C* = CH), 134.9 (C_q, Ar-*C*), 129.4 (+, Ar-*C*), 129.3 (C_q, Ar-*C*), 128.9 (+, 2×Ar-*C*), 127.4 (+, 2×Ar-*C*), 122.3 (+, HC = CH), 117.9 (+, Ar-*C*), 115.3 (+, Ar-*C*), 114.3 (+, Ar-*C*), 102.5 (C_q, Ar-*C*), 94.9 (+, Ar-*C*), 94.1 (+, Ar-*C*), 78.6 (+, *CH*), 67.9 (-, OCH_2), 42.1 (-, CH_2), 38.2 (-, NCH_2), 25.9 (-, CH_2), 25.6 (-, CH_2) ppm. – ESI-MS $[C_{28}H_{27}NO_7+H]^+$: *m/z* calcd 490.18; found 490.20. – MP 164 °C dec.

Luteolin-cinnamic acid amide (N-(4-((2-(3,4-dihydroxyphenyl)-5-hydroxy-4-oxo-4H-chromen-7-yl)oxy)butyl)cinnamamide)

The product was obtained as yellow solid in 15% yield (11 mg).

^{1}H NMR: (400 MHz, DMSO-d_6): δ = 12.96 (s, 1H, O*H*), 8.15 (t, ^3J = 5.7 Hz, 1H, N*H*), 7.55 (m, 2H), 7.46–7.33 (m, 6H), 6.89 (d, ^3J = 8.1 Hz, 1H, Ar-*H*), 6.74–6.69 (m, 2H, C=C*H*, Ar-*H*), 6.63 (d, $^3J_{trans}$ = 15.8, 1H), 6.36 (d, ^4J = 2.2 Hz, 1H, Ar-*H*), 4.13 (t, ^3J = 6.6 Hz, 2H, OCH_2), 3.33–3.22 (q, ^3J = 6.5 Hz, 2H, NC*H*), 1.78 (m, 2H, CH_2), 1.64 (m, 2H, CH_2) ppm. – ^{13}C NMR (100 MHz, DMSO-d_6): δ 181.7 (C_q, *C*=O), 164.8 (NC=O), 164.4 (C_q, Ar-*C*), 164.2 (C_q, Ar-*C*), 161.1 (C_q, Ar-*C*), 157.2 (C_q, Ar-*C*), 146.9 (C_q, Ar-*C*), 145.8 (C_q, Ar-*C*), 138.4 (+, H*C*=CH), 134.9 (C_q, Ar-*C*), 129.3 (+, Ar-*C*), 128.9 (+, 2×Ar-*C*), 127.4 (+, 2×Ar-*C*), 122.2 (+, H*C*=CH), 121.3 (C_q, Ar-*H*), 119.9 (+, Ar-*C*), 115.9 (+, Ar-*C*), 113.4 (+, Ar-*C*), 104.5 (C_q, Ar-*C*), 102.9 (+, Ar-*C*), 98.3 (+, Ar-*C*), 92.9 (+, Ar-*C*), 68.1 (-, OCH_2), 38.2 (-, NCH_2), 25.9 (-, CH_2), 25.6 (-, CH_2) ppm. – ESI-MS $[C_{28}H_{25}NO_7+H]^+$: *m/z* calcd 488.17; found 488.20. – MP 209 °C.

Fustin-cinnamic acid amide (N-(4-((2-(3,4-dihydroxyphenyl)-3-hydroxy-4-oxochroman-7-yl)oxy)butyl)cinnamamide)

The product was obtained as off- colourless solid in 11% yield (5 mg).

^{1}H NMR: (400 MHz, DMSO-d_6): δ = 8.13 (s, 1H, t, ^3J = 5.6 Hz, 1H, N*H*), 7.69 (d, ^3J = 8.8 Hz, 1H, Ar-*H*), 7.58–7.51 (m, 2H, Ar-*H*), 7.44–7.34 (m, 4H, 3×Ar-*H*, C=C*H*), 6.89 (d, ^4J = 2.0 Hz, 1H, Ar-*H*), 6.76 (dd, ^3J = 8.16, ^4J = 1.9 Hz, 1H, Ar-*H*), 6.73 (d, *J* = 8.16 Hz, 1H, Ar-*H*), 6.67 (dd, ^3J = 8.8, ^4J = 2.3 Hz, 1H, Ar-*H*), 6.61 (d, $^3J_{trans}$ = 15.9 Hz, 1H, C=C*H*), 6.56 (d, ^4J = 2.3 Hz, 1H, Ar-*H*), 5.01 (d, ^3J = 11.4 Hz, 1H, C*H*), 4.45 (d, ^3J = 11.4 Hz, 1H, C*H*), 4.08 (t, ^3J = 6.6 Hz, 2H, OCH_2), 3.24 (m, 2H, NCH_2), 1.76-1.72 (m, 2H, CH_2), 1.64 – 1.55 (m, 2H, CH_2) ppm. – ^{13}C NMR (100 MHz, DMSO-d_6): δ 192.6 (C_q, *C*=O), 165.0 (C_q, Ar-*C*), 164.8 (C_q, N*C*=O), 162.8 (C_q, Ar-*C*), 145.8 (C_q, Ar-*C*), 144.9 (C_q, Ar-*C*), 138.4 (+, H*C*=CH), 134.9 (C_q, Ar-*C*), 129.3 (+ Ar-*C*), 128.8 (+, 2×Ar-*C*), 128.2 (+, Ar-*C*), 127.4 (+, 2×Ar-*C*), 125.5 (C_q, Ar-*C*), 122.3 (+, H*C*=CH), 119.5 (+, Ar-*C*), 115.3 (+, Ar-*C*), 115.0 (+, Ar-*C*), 114.4 (C_q, Ar-*C*), 110.4 (+, Ar-*C*), 101.2 (+, Ar-*C*), 83.6 (+, *C*H), 72.5 (+, *C*H), 67.8 (-, OCH_2), 38.2 (-, NCH_2), 25.9 (-, CH_2), 25.7 (-, CH_2) ppm. – ESI-MS $[C_{28}H_{27}NO_7+H]^+$: *m/z* calcd 490.18; found 490.15. – MP 169 °C.

Fisetin-cinnamic acid amide (N-(4-((2-(3,4-dihydroxyphenyl)-3-hydroxy-4-oxo-4H-chromen-7-yl)oxy)butyl)cinnamamide)

The product was obtained as yellow solid in 12% yield (12 mg).

^{1}H NMR: (400 MHz, DMSO-d_6): δ = 9.23 (s, 2H, O*H*), 8.15 (t, ^3J = 5.2 Hz, 1H, N*H*), 7.91 (d, 1H, ^3J = 8.5 Hz, Ar-*H*), 7.70 (d, ^4J = 2.2 Hz, 1H, Ar-*H*), 7.62 (dd, 1H, ^{3}J = 8.6, ^4J = 2.2 Hz, 7.56–7.53 (m, 3H, 3×Ar-*H*,), 7.45–7.35 (m, 4H, Ar-*H*, *H*C=CH), 7.07 (d, 1H, ^3J = 8.7 Hz, Ar-*H*), 6.87 (d, 1H, ^4J = 2.2 Hz, Ar-*H*), 6.63 (d, $^3J_{trans}$ = 15.8 Hz, 1H, HC=C*H*), 4.08 (t, ^3J = 6.3 Hz, 2H, OCH_2), 3.27 (q, ^3J = 6.5 Hz, 2H, NC*H*), 1.80 (m, 2H, CH_2), 1.65 (m, 2H, CH_2) ppm. – ^{13}C NMR (100 MHz, DMSO-d_6): δ 171.9 (C_q, *C*=O), 164.8 (N*C*=O), 162.7 (C_q, Ar-*C*), 156.4 (C_q, Ar-*C*), 156.2 (C_q, Ar-*C*), 148.1 (C_q, Ar-*C*), 146.5 (C_q, Ar-*C*), 145.4 (C_q, Ar-*C*), 138.4 (+, H*C*=CH), 134.9 (C_q, Ar-*C*), 129.3 (+, Ar-*C*), 128.8 (+, 2×Ar-*C*), 127.4 (+, 2×Ar-*C*), 126.4 (+, Ar-*C*), 122.3 (+, H*C*=CH), 121.8 (C_q, Ar-*C*), 119.3 (+, Ar-*C*), 115.5 (+, Ar-*C*), 114.5 (+, Ar-*C*), 113.8 (C_q, Ar-*C*), 112.9 (+, Ar-*C*), 101.7 (+, Ar-*C*), 67.9 (-, OCH_2), 38.3 (-, NCH_2), 26.1 (-, CH_2), 25.8 (-, CH_2) ppm. – ESI-MS $[C_{28}H_{25}NO_7+H]^+$: *m/z* calcd 488.16; found 488.15– MP 218 °C.

BiologyCell Culture general procedures

HT22 cells were grown in Dulbecco's Modified Eagle Medium (DMEM, Sigma Aldrich, Munich Germany) supplemented with 10% (v/v) fetal calf serum (FCS) and 1% (v/v) penicillin-streptomycin. BV-2 cells were grown in low glucose DMEM (Invitrogen, Carlsbad, CA, USA) supplemented with 10% FCS and 1% (v/v) penicillin-streptomycin. Cells were subcultured every two days and incubated at 37 °C with 5% CO_2 in a humidified incubator.

Compounds were dissolved in dimethyl sulfoxide (DMSO, Sigma Aldrich, Munich, Germany) as stock solutions and diluted further into culture medium.

For determination of cell viability, a colorimetric 3-(4,5-dimethylthiazol-2-yl)-2,5-diphenyl tetrazolium bromide (MTT, Sigma Aldrich, Munich, Germany) assay was used. MTT solution (4 mg/mL in PBS) was diluted 1:10 with medium and added to the wells after removal of the old medium. Cells were incubated for 3 hours and then lysis buffer (10% SDS) was applied. The next day, absorbance at 560 nm was determined with a multiwell plate photometer (Tecan, SpectraMax 250).

Oxytosis in HT22 cells

HT22 cells were seeded into sterile 96-well plates at a density of 5×10^3 per well and incubated overnight. The medium was exchanged, and cells were treated with 5 mM glutamate (monosodium-*L*-glutamate, Sigma Aldrich, Munich, Germany) alone or together with 1.56, 3.12, 6.25 or 12.5 μM of the respective compound. After 24 hours cell viability was determined using a colorimetric MTT assay as described above. Results are presented as percentage of untreated control cells. Data is expressed as means ± SEM of three independent biological experiments. Each biological experiment contained three technical replicates. Analysis was accomplished using GraphPad Prism 5 Software applying Oneway ANOVA followed by Dunnett's multiple comparison posttest. Levels of significance: * $p<0.05$; ** $p<0.01$; *** $p<0.001$.

Reactive oxygen species (ROS) measurement

HT22 cells were seeded into sterile black walled 96-well plates at a density of 5×10^3 per well and incubated overnight. The medium was exchanged, and cells were treated with 5 mM glutamate (monosodium-*L*-glutamate, Sigma Aldrich, Munich, Germany) alone or together with 1.56, 3.12, 6.25 or 12.5 μM of the respective compound for 6 hours. The medium was removed and 100 μL phenol red-free Hank's balanced salt solution (Sigma Aldrich, Munich, Germany) containing 1 μM CM-H_2DCFDA (Thermo Fisher Scientific, Darmstadt, Germany) was added. After 20 min incubation, fluorescence (λ excitation = 495 nm, λ emission = 525 nM) was determined using a Tecan Infinite M Plus microplate reader or subjected to fluorescence microscopy using a Zeiss Axiovert Observer fluorescence microscope. Fluorescence was normalized to control cells not exposed to glutamate. Images were processed with the ZEN 3.4 (blue edition) software. Data is expressed as means ± SEM of three independent biological experiments. Each biological experiment contained three technical replicates. Analysis was accomplished using GraphPad Prism 5 Software applying Oneway ANOVA followed by Dunnett's multiple comparison posttest. Levels of significance: */# $p<0.05$; **/## $p<0.01$; ***/### $p<0.001$.

Ferroptosis in HT22 cells

HT22 cells were seeded into sterile 96-well plates at a density of 3×10^3 per well and incubated overnight. The medium was exchanged, and cells were treated with 300 nM RSL-3 (Sigma Aldrich, Munich, Germany) alone or together with 1.56, 3.12, 6.25 or 12.5 μM of the respective compound. After 24 hours cell viability was determined using a colorimetric MTT assay as described above. Results are presented as percentage of untreated control cells. Data is expressed as means ± SEM of three independent biological experiments. Each biological experiment contained three technical replicates. Analysis was accomplished using GraphPad Prism 5 Software applying Oneway ANOVA followed by Dunnett's multiple comparison posttest. Levels of significance: * $p<0.05$; ** $p<0.01$; *** $p<0.001$.

ATP depletion in HT22 cells

HT22 cells were seeded into sterile 96-well plates at a density of 3×10^3 per well and incubated overnight. The medium was exchanged, and cells were treated with 17.5 μM iodoacetic acid (IAA) (Sigma Aldrich, Munich, Germany) alone or together with 1.56, 3.12, 6.25 or 12.5 μM of the respective compound. After 24 hours cell viability was determined using a colorimetric MTT assay as described above. Results are presented as percentage of untreated control cells. Data is expressed as means ± SEM of three independent biological experiments. Each biological experiment contained three technical replicates. Analysis was accomplished using GraphPad Prism 5 Software applying Oneway ANOVA followed by Dunnett's multiple comparison posttest. Levels of significance: * $p<0.05$; ** $p<0.01$; *** $p<0.001$.

Cellular uptake experiments and stability in cell culture medium

BV-2 cells or HT22 cells were grown in sterile 100 mm dishes at a density of 8×10^6 cells overnight. The next day, 50 μM taxifolin-CA diluted in cell culture medium (4 mL) was added. Cells were incubated for the indicated time periods, after which the supernatant was removed, and cells were washed twice with PBS. Further PBS (1 mL) was added, cells were scraped and transferred to Eppendorf tubes. The samples were centrifuged (10000 × g for 5 minutes) and resuspended in 200 μL of MeOH. The cells were frozen in liquid nitrogen and thawed at 37 °C (10 times). Cell debris was pelleted by centrifugation (10000 × g for 10 minutes) and the supernatant was collected for HPLC analysis using the HPLC system described above equipped with a Synergi 4 U fusion-RP (250 mm × 10 mm) column as a stationary phase. As a mobile phase, a gradient of methanol/water with 0.1% (v/v) formic acid. Parameters: A = water, B = methanol, V(B)/(V(A) + V(B)) = from 5% to 80% over 20 min, V(B)/(V(A) + V(B)) = 80% for 10 min, V(B)/(V(A) + V(B)) = from 80% to 5% over 5 min. The method was performed with a flow rate of 1.0 mL/min and the injection volume was 50 μL.

For stability experiments, taxifolin-CA was diluted in Dulbecco's Modified Eagle Medium (DMEM, Sigma Aldrich, Munich Germany) supplemented with 10% (v/v) fetal calf serum (FCS) and 1% (v/v) penicillin-streptomycin to a final concentration of 50 μM and incubated for the indicated time period at 37 °C in an Eppendorf Thermo Mixer F1.5. The solution was mixed 1/1 with ice-cold methanol and precipitant was removed by centrifugation (10000 × g for 10 minutes). The supernatant was subjected to HPLC-UV/MS analysis and quantification was done by calibration curve (cf. Supporting Information).

Neuroprotection in vivo

Animals. Male Swiss mice 6 weeks old, body weight 30–40 g, obtained from JANVIER (Saint Berthevin, France) were housed in the animal facility of the University of Montpellier (CECEMA, Office of Veterinary Services agreement # B-34-172-23) with access to food and water ad libitum (except during behavioral tests). The humidity and temperature were controlled, and the mice were kept at a 12 h light / 12 h dark cycle (lights off at 7:00 p.m.). All animal procedures were conducted in strict adherence to the European Union directives of September 22nd, 2010 (2010/63/UE) and to the ARRIVE guidelines. The project was authorized by the French National Ethics Committee (APAFIS #1485-15034). Animals were assigned to different treatment groups randomly.

Preparation of compound injections. Compounds was dissolved in 100% DMSO at a concentration of 6 mg/mL to give a stock solution, which was diluted with saline (0.9% NaCl in milliQ water) and DMSO to the final test concentration and a final percentage of 60% DMSO. 60% DMSO in saline served as the vehicle (V2). After compound injections, the behavior of the mice in their home cage was checked visually. Weight was examined once per day. As shown in Figure S5, the peptide injection resulted in a ~1 g drop on day 2 of treatment but then animals recovered weight gain and the drug treatments failed to affect this increase as compared to $A\beta_{25\text{-}35}$ + V2 treated mice, with the notable exception of the quercetin (0.3 mg/Kg IP) group that indeed did not show the $A\beta_{25\text{-}35}$-induced weight drop on day 2 (Figure S5).

Amyloid peptide preparation and ICV injection. All experiments followed previously described protocols.[8b,13,23] The $A\beta_{25\text{-}35}$ peptide was prepared according to Maurice et al.[13] Mice were anesthetized with 2.5% isoflurane. Then, oligomerized $A\beta_{25\text{-}35}$ peptide (9 nmol in 3 μL/mouse) was injected intracerebroventricularly. Bidistilled water was used as a vehicle (V1).

Spontaneous alternation performance in a Y-maze. On day 8 of the study, the spatial working memory of all mice was evaluated in the Y-maze. The Y-maze is made from grey polyvinylchloride and has three identical arms (length 40 cm, height 13 cm, bottom width 3 cm, top width 10 cm (walls converge at an equal angle). For evaluation of memory, every mouse was placed into one arm and was allowed to explore the maze for 8 min. All entries into an arm (including the return into the same arm) were counted and the number of alternations (mouse entered all three arms consecutively) was calculated as percentage of total number of arm entries [alternations / (arm entries-2)*100].

Step-through passive avoidance test. The test was performed on day 9 and day 10 in a two-compartment box [width 10 cm, total length 20 cm (10 cm per compartment), height 20 cm] consisting of polyvinylchloride. One of the compartments was white and illuminated with a bulb (60 W, 40 cm above the center of the compartment), the second compartment was black, covered, and had a grid floor. A guillotine door separated the compartments. On day 9 (training), each animal was placed in the white compartment and was left to explore for 5 s. Then, the door was opened, which allowed the mouse to enter the black compartment. After it had entered, the door was closed, and a foot shock was delivered (0.3 mA) for 3 s generated by a scramble shock generator (Lafayette Instruments, Lafayette, USA). The step-through latency (time the mouse spent in the white compartment after the door was opened) and the level of sensitivity (no sign = 0, flinching reactions = 1, vocalization = 2) were recoded. Treatment with sterubin (1) did not affect the measured parameters. On the next day (day 10), each mouse was placed in the white compartment and was allowed to explore for 5 s. Then, the door was opened allowing the mouse to

step over into the black compartment. The step-through latency was measured for up to 300 s.

Sacrifice and brain collection. All animals were sacrificed on day 11. The brains were collected, hippocampus and cortex were isolated, and the samples were frozen at −80 °C.

Statistical analysis. Data were analyzed by the software GraphPad Prism 9.0 software. Weight gain and alternation percentages were analyzed using one-way ANOVA, followed by Dunnett's post-hoc multiple comparison test. Passive avoidance retention had a maximum step-through latency of 300 s. Therefore, a Gaussian distribution could not be assumed. The results were analyzed using a Kruskal-Wallis non-parametric ANOVA, followed by a Dunn's multiple comparison test. $p < 0.05$ was considered as statistically significant.

Acknowledgements

We thank Professor Dr. Pamela Maher (Cellular Neurobiology Laboratory, The Salk Institute for Biological Studies, La Jolla, U.S.A.) for providing HT22 and BV-2 cells. We also thank the CECEMA animal facility (University of Montpellier, France). M.D. and T.M. acknowledge the Franco-Bavarian University Cooperation Center under FK03-2020. P. S. acknowledges a PhD position awarded within the International Doctoral Program "Receptor Dynamics" by the Elite Network of Bavaria. Open Access funding enabled and organized by Projekt DEAL.

Conflict of Interest

The authors declare no conflict of interest.

Data Availability Statement

The data that support the findings of this study are available in the supplementary material of this article.

Keywords: AD mouse modele · Alzheimer's diseas · natural product hybrids · oxytosis/ferroptosis

[1] S. Przedborski, M. Vila, V. Jackson-Lewis, *J. Clin. Invest.* **2003**, *111*, 3–10.
[2] C. A. Lane, J. Hardy, J. M. Schott, *Eur. J. Neurol.* **2018**, *25*, 59–70.
[3] P. Maher, *Int. J. Mol. Sci.* **2019**, *20*.
[4] B. J. Andreone, M. Larhammar, J. W. Lewcock, *Cold Spring Harbor Perspect. Biol.* **2020**, *12*, a036434.
[5] P. Patil, A. Thakur, A. Sharma, S. J. S. Flora, *Drug Dev. Res.* **2020**, *81*, 165–183.
[6] D. J. Newman, G. M. Cragg, *J. Nat. Prod.* **2020**, *83*, 770–803.
[7] F. Pohl, P. Kong Thoo Lin, *Molecules* **2018**, *23*, 3283.
[8] a) S. Schramm, G. Huang, S. Gunesch, F. Lang, J. Roa, P. Högger, R. Sabaté, P. Maher, M. Decker, *Eur. J. Med. Chem.* **2018**, *146*, 93–107; b) S. Gunesch, C. Kiermeier, M. Hoffmann, W. Fischer, A. F. M. Pinto, T. Maurice, P. Maher, M. Decker, *Redox Biol.* **2019**, 101378; c) J. Vrba, R. Gažák, M. Kuzma, B. Papoušková, J. Vacek, M. Weiszenstein, V. Křen, J. Ulrichová, *J. Med. Chem.* **2013**, *56*, 856–866.
[9] S. Gunesch, D. Soriano-Castell, S. Lamer, A. Schlosser, P. Maher, M. Decker, *ACS Chem. Neurosci.* **2020**, *11*, 3823–3837.
[10] S. Schramm, S. Gunesch, F. Lang, M. Saedtler, L. Meinel, P. Högger, M. Decker, *Arch. Pharm. Chem. Life Sci.* **2018**, *351*, 1800206.
[11] A. Mattarei, L. Biasutto, F. Rastrelli, S. Garbisa, E. Marotta, M. Zoratti, C. Paradisi, *Molecules* **2010**, *15*, 4722–4736.
[12] M. Prior, C. Chiruta, A. Currais, J. Goldberg, J. Ramsey, R. Dargusch, P. A. Maher, D. Schubert, *ACS Chem. Neurosci.* **2014**, *5*, 503–513.
[13] T. Maurice, B. P. Lockhart, A. Privat, *Brain Res.* **1996**, *706*, 181–193.
[14] H. Wagner, L. Farkas, in *The Flavonoids* (Eds.: J. B. Harborne, T. J. Mabry, H. Mabry), Springer US, Boston, MA, **1975**, pp. 127–213.
[15] B. Roschek, R. C. Fink, M. D. McMichael, D. Li, R. S. Alberte, *Phytochemistry* **2009**, *70*, 1255–1261.
[16] H. Aft, *J. Org. Chem.* **1965**, *30*, 897–901.
[17] a) T. H. Murphy, M. Miyamoto, A. Sastre, R. L. Schnaar, J. T. Coyle, *Neuron* **1989**, *2*, 1547–1558; b) S. Tan, M. Wood, P. Maher, *J. Neurochem.* **1998**, *71*, 95–105.
[18] S. Tan, D. Schubert, P. Maher, *Curr. Top. Med. Chem.* **2001**, *1*, 497–506.
[19] P. Maher, A. Currais, D. Schubert, *Cell Chem. Biol.* **2020**, *27*, 1456–1471.
[20] M. Oparka, J. Walczak, D. Malinska, L. M. P. E. van Oppen, J. Szczepanowska, W. J. H. Koopman, M. R. Wieckowski, *Methods* **2016**, *109*, 3–11.
[21] U. Saxena, *Expert Opin. Ther. Targets* **2012**, *16*, 351–354.
[22] P. Maher, K. F. Salgado, J. A. Zivin, P. A. Lapchak, *Brain Res.* **2007**, *1173*, 117–125.
[23] a) M. Hoffmann, C. Stiller, E. Endres, M. Scheiner, S. Gunesch, C. Sotriffer, T. Maurice, M. Decker, *J. Med. Chem.* **2019**, *62*, 9116–9140; b) T. Maurice, M. Strehaiano, N. Siméon, C. Bertrand, A. Chatonnet, *Behav. Brain Res.* **2016**, *296*, 351–360; c) M. Scheiner, A. Sink, M. Hoffmann, C. Vrigneau, E. Endres, A. Carles, C. Sotriffer, T. Maurice, M. Decker, *J. Am. Chem. Soc.* **2022**, *144*, 3279–3284; d) J. Hofmann, S. Fayez, M. Scheiner, M. Hoffmann, S. Oerter, A. Appelt-Menzel, P. Maher, T. Maurice, G. Bringmann, M. Decker, *Chem. Eur. J.* **2020**, *26*, 7299–7308.
[24] P. B. Reiner, A. G. Laycock, C. J. Doll, *Neurosci. Lett.* **1990**, *119*, 175–178.
[25] J. Baell, M. A. Walters, *Nature* **2014**, *513*, 481–483.
[26] a) J. B. Baell, *J. Nat. Prod.* **2016**, *79*, 616–628; b) S. C. Owen, A. K. Doak, P. Wassam, M. S. Shoichet, B. K. Shoichet, *ACS Chem. Biol.* **2012**, *7*, 1429–1435.
[27] P. Maher, *Genes Nutr.* **2009**, *4*, 297.
[28] W. Fischer, A. Currais, Z. Liang, A. Pinto, P. Maher, *Redox Biol.* **2019**, *21*, 101089.
[29] T. E. Huntley, J. K. Neitzel, M. K. Elson, *Biochim. Biophys. Acta Mol. Prot. Struc.* **1977**, *490*, 112–119.
[30] R. M. Weinshilboum, D. M. Otterness, C. L. Szumlanski, *Annu. Rev. Pharmacool. Toxicol.* **1999**, *39*, 19–52.
[31] a) B. T. Zhu, E. L. Ezell, J. G. Liehr, *J. Biol. Chem.* **1994**, *269*, 292–299; b) Z. Chen, M. Chen, H. Pan, S. Sun, L. Li, S. Zeng, H. Jiang, *Drug Metab. Dispos.* **2011**, *39*, 667; c) Y. Cao, Z.-J. Chen, H.-D. Jiang, J.-Z. Chen, *J. Phys. Chem. B* **2014**, *118*, 470–481.
[32] a) J. P. Ley, G. Krammer, G. Reinders, I. L. Gatfield, H.-J. Bertram, *J. Agric. Food Chem.* **2005**, *53*, 6061–6066; b) T. Geissman, *J. Am. Chem. Soc.* **1940**, *62*, 3258–3259.
[33] C. Hu, Z. Zhou, Y. Xiang, X. Song, H. Wang, K. Tao, X. Ye, *Med. Chem. Res.* **2018**, *27*, 194–205.
[34] E. Kiehlmann, M. G. Szczepina, *Cent. Eur. J. Chem.* **2011**, *9*, 492–498.
[35] S. Rubio, J. Quintana, M. López, J. L. Eiroa, J. Triana, F. Estévez, *Eur. J. Pharmacol.* **2006**, *548*, 9–20.
[36] a) T. K.-D. Hoang, T. K.-C. Huynh, T.-D. Nguyen, *Bioorg. Chem.* **2015**, *63*, 45–52; b) Y.-Q. Li, F. Yang, L. Wang, Z. Cao, T.-J. Han, Z.-A. Duan, Z. Li, W.-J. Zhao, *Eur. J. Med. Chem.* **2016**, *112*, 196–208.
[37] E. Kiehlmann, *Org. Prep. Proced. Int.* **1999**, *31*, 87–97.

Manuscript received: March 11, 2022
Version of record online: May 27, 2022